RM E53K30

NACA RM E53K30

NACA

RESEARCH MEMORANDUM

FLAME QUENCHING BY A VARIABLE-WIDTH RECTANGULAR-SLOT BURNER AS A FUNCTION OF PRESSURE FOR VARIOUS PROPANE-OXYGEN-NITROGEN MIXTURES

By Abraham L. Berlad

Lewis Flight Propulsion Laboratory
Cleveland, Ohio

NATIONAL ADVISORY COMMITTEE FOR AERONAUTICS

WASHINGTON

January 28, 1954

NACA RM E53K30

NATIONAL ADVISORY COMMITTEE FOR AERONAUTICS

RESEARCH MEMORANDUM

FLAME QUENCHING BY A VARIABLE-WIDTH RECTANGULAR-SLOT BURNER AS A FUNCTION OF PRESSURE FOR VARIOUS PROPANE-OXYGEN-NITROGEN MIXTURES

By Abraham L. Berlad

SUMMARY

Flame quenching by a variable-width rectangular-slot burner as a function of pressure for various propane-oxygen-nitrogen mixtures was investigated. It was found that for cold gas temperatures of 27° C, for pressures of 0.1 to 1.0 atmosphere, and for volumetric oxygen fractions of the oxidant of 0.17, 0.21, 0.30, 0.50, and 0.70, the relation between pressure p and quenching distance d is given by $d \propto p^{-r}$, with $r = 1$, for equivalence ratios approximately equal to one. For the complete range of equivalence ratios studied, it was found that $0.60 \leq r \leq 1.12$.

The quenching theory of Simon and Belles was used to predict values of r for the range of pressures and $O_2/(O_2 + N_2)$ ratios encountered in this study. For equivalence ratios less than or equal to unity, the predicted value of r deviated from the observed value by an average of 7.1 percent. For equivalence ratios greater than unity, this deviation increased to 13.6 percent. It was further shown, for equivalence ratios less than or equal to unity, that an equation based on a diffusion mechanism and containing one empirical constant may be successfully used to predict the observed quenching distance within 4.2 percent. The equation in its present form does not appear to be suitable for values of the equivalence ratio greater than unity.

A theoretical investigation has also been made of the error implicit in the assumption that flame quenching by plane parallel plates of infinite extent is equivalent to that by a rectangular burner. A curve is presented which relates quantitatively the magnitude of this error to the length-to-width ratio of the rectangular burner. It is shown that a length-to-width burner ratio of 10, or more, involves a difference in the quenching distances, as measured in these two ways, of 3 percent or less.

INTRODUCTION

The quenching of a flame by a channel of a given size and shape is an easily measured phenomenon which may supply much information relating to the many other associated flame phenomena. Thus, the distance of closest approach of a flame to a cold wall, the minimum ignition energy, the relative ability of a stable flame to generate a large amount of heat per unit volume per unit time, the critical conditions of container geometry, pressure, and temperature under which this flame can or cannot exist may all be related to the quenching distance. The quenching distance itself varies with fuel type, oxidant type, fuel-oxidant ratio, quenching surface geometry, temperature, and total pressure.

Several quantitative attempts to relate quenching distance to the fundamental properties characterizing the combustion wave have been made. Lewis and von Elbe (ref. 1) have related quenching distance to minimum ignition energy and burning velocity by assuming that a consideration of heat-transfer processes alone is sufficient to explain the behavior of the combustion wave. No thorough test of this theory has been made, chiefly because of the lack of low-pressure burning-velocity data. A quenching theory is proposed in reference 2 in which the diffusion of H, O, and OH radicals in the flame front plays the vital role in determining whether or not the flame will be quenched by a given wall geometry. This latter theory can be readily applied (once flame equilibrium radical concentrations are calculated) and has been successful in predicting quenching distances for propane-air, ethylene-air, and isooctane-air flames over a range of pressures. In addition, reference 2 gives a relation between quenching distance as defined by the separation distance of plane parallel plates of infinite extent and that defined by the diameter of a cylinder.

The work herein reported is part of a flame-propagation investigation which was performed at the NACA Lewis laboratory with a water-cooled rectangular-slot burner to measure the quenching of propane-oxygen-nitrogen flames over a range of pressures, oxygen content of the oxidant, and fuel-oxidant ratio.

The objectives of this investigation were:

(1) To provide the data necessary to describe the wall quenching of propane-oxygen-nitrogen flames as a function of fuel-oxidant ratio, oxygen content of the oxidant, and pressure

(2) To treat these data in the light of current theoretical concepts of flame quenching and thus help to establish those relations which may properly serve to emphasize the important processes taking place in the combustion wave and which may thus prove useful in predicting quenching distances and other flame phenomena over a large range of conditions

(3) To consider quantitatively the errors involved in the often-made assumption that a rectangular-slot burner of various length-to-width ratios has the same quenching action as a narrow slit of infinite length

EXPERIMENTAL DETAILS

Quenching-distance burner. - The quenching-distance burner used in making these measurements is shown in figure 1. The burner was made of stainless steel. The desired fuel-oxidant mixture was introduced through three inlets located at the bottom of the burner channel and designated A. Fine glass beads B were sandwiched between two layers of 200-mesh stainless steel screen which served both as a flow straightener and as a flame arrestor. The jacketed walls of the burner were kept at 40° C by circulating water. This wall temperature was sufficiently high to prevent condensation of water on the burner lip. The burner length was 5 inches and the slit width, established by adjusting the movable burner-lip assembly, was never more than 1/2 inch. Two inside-thickness gages were used at the ends of the rectangular slot to determine the burner wall separation. A spark ignitor was used to establish a flame atop the rectangular burner port. A thermocouple C was employed to measure local temperatures and to indicate flash back of the flame through the rectangular channel of the burner.

Flow system. - A schematic diagram of the quenching distance setup is shown in figure 2. Two similar injection and metering sections were used for the oxidant and fuel. The tanked O_2-N_2 mixtures A and the tanked propane B each passed through separate pressure-regulation and filtering stages, C and D, respectively. Critical flow orifices E were used to meter both oxidant and fuel. Solenoid valves F were both either fully open or fully closed. Fuel and oxidant were mixed just ahead of the valve G and flame arrestor H and then fed into the quenching-distance burner J. The quenching-distance burner was situated in a four-windowed, pressure-tight burner chamber I of 3.5-cubic-foot capacity. The pressure in the burner chamber was given by a mercury manometer M. The burner exhaust L led to a cold trap O and then to a 40-cubic-foot-capacity plenum P. The pressure in I was regulated by first adjusting the throttling valve just ahead of the 34-cubic-foot-per-minute exhaust pump. The desired pressure was then obtained by adjusting the room air or nitrogen bleed K or by injection of service air N into the exhaust.

Gas mixtures. - Oxygen-nitrogen mixtures for which $\alpha = O_2/(O_2 + N_2)$ (volumetric oxygen fraction) was 0.17, 0.21, 0.30, 0.50, and 0.70 were used as oxidants. The supplier's stated accuracy for these oxidants was ±0.1 percent O_2. The propane used in these experiments had a stated purity of 99.9 percent.

Procedure. - Quenching data were obtained in the following way. Inside-thickness gages were used to establish and measure the burner-wall separation. The burner chamber I was then closed. The exhaust pump was started and properly throttled. Air flow through K or N was used to stabilize the burner pressure in the region of interest. Solenoids F were opened and pressure regulators C adjusted to provide critical flows through the two orifices E. The desired fuel-oxidant mixture was then ignited at the burner port. Pressure and temperature upstream of the fuel and oxidant orifices were recorded. The combustion pressure, in I, was stabilized and recorded. The determination of whether or not the given fuel-oxidant mixture, burning at a given pressure, would be quenched by a rectangular channel of known dimensions and temperature was made as follows. Solenoids F were simultaneously and suddenly closed. The flame seated on the burner would then either die on the burner lip or flash back through the rectangular burner channel. Flash back was detected by a thermocouple at the bottom of the channel. If flash back did occur, the pressure was lowered and stabilized at a somewhat reduced level and the experiment repeated until a pressure was reached at which no flash back occurred. Conversely, if flash back did not occur, the pressure was raised and stabilized at a somewhat higher level and the experiment repeated until a pressure was reached at which flash back did occur. The test procedure was then continued and the limiting pressure taken to be the highest pressure at which flash back did not occur.

Experimental errors. - The uncertainty in the determination of pressure limits for a given fuel-oxidant ratio and quenching distance was 0.02 inch of mercury or 6.7×10^{-4} atmosphere. This corresponds to a maximum error of 0.7 percent in the pressure limit, at a pressure of 0.1 atmosphere. Added to this error, however, were the ones arising from uncertainties in the fuel and oxidant flows and in the burner-wall separation. The uncertainty in the calibration of the critical flow orifices was ±1 percent. Further, the uncertainty in reading the pressure and temperature, upstream of the critical flow orifices, introduced an additional error in the flow having a maximum value of 0.5 percent. The uncertainty in the quenching distance was ±0.001 inch. The error in the pressure limits caused by uncertainties in determining oxidant-fuel ratio varied from very small near the minimum of the p against O/F curve (fig. 5) to fairly large where the curve is steep. Similarly, the error in the pressure limit caused by uncertainties in the measurement of the burner spacing is greater for small openings (high pressure and oxygen concentrations) and less for large openings (low pressures and oxygen concentrations). It is estimated from the general reproducibility of the data that the average error in the pressure limit is ±2 percent.

GEOMETRICAL CONSIDERATIONS

In reference 2, the average chain-length calculations of Semenoff (ref. 3) are used to derive expressions for the quenching distance associated with plane parallel plates and with cylindrical tubes. The ratio of plane-parallel-plate and cylindrical-tube quenching distances is calculated to be 0.61. In practice, of course, the case of the infinitely long, plane-parallel-wall burner is approximated by a rectangular-slot burner. A comparison of the propane-air rectangular-slot-burner quenching data of Friedman and Johnston (ref. 4) with the cylindrical-tube data of reference 5 was made (ref. 2), and the average ratio of the quenching distances was found to be 0.70 as compared with the theoretically predicted value, for the ideal case, of 0.61. At least part of this difference may be attributed to the "end effects" associated with the rectangular-slot burner. It is also evident that these end effects depend upon the length-to-width ratio of the burner slot. Length-to-width ratios as low as 3.6 were, on occasion, employed in obtaining the data of reference 4.

In order to calculate the quenching effect for a given rectangular-slot-burner geometry, it is necessary to consider the effect the slot geometry can have on the flame. Fortunately, the criteria which affect the slot geometry end effects appear to be independent of the theory employed to calculate them since the differential equations and the boundary conditions which characterize the interaction of the wall with the flame are formally the same whether the wall acts as a radical sink (diffusion theory) or as a heat sink (thermal theory). In one case, the equations describe the spatial distribution of the concentration of active particles which are generated uniformly through the volume and which are destroyed upon collision with the boundary. In the other case, the equations describe the spatial distribution of the flame temperature in a region where heat is being generated uniformly throughout the volume and lost by conduction to the constant-temperature walls.

The effect of slot geometry on the flame has been calculated with the use of the diffusion equation (appendix B). The results presented in figure 3 show that if the length-to-width ratio of a rectangular burner is kept at 10, or greater, the error involved in assuming the apparatus to consist of plane parallel walls of infinite extent is 3 percent or less. This condition was satisfied in this investigation. Figure 3 shows the error incurred in making the assumption that the slot is infinitely long. Thus, for a rectangular burner where $b/d_r = 3.6$ (one of the values encountered in ref. 4), the error involved is 9 percent. The value $d_p/d_c = 0.61$ (ref. 2) may be combined with the d_p/d_r values of figure 3 to construct figure 4, where d_r/d_c is plotted against d_r/b for the range $0 \leqq (d_r/b) \leqq 1$. It is thus evident that quenching data obtained through the use of a rectangular-slot burner of variable length-to-width ratios should, if these data are to be considered as plane-parallel-wall data, either represent cases where end effects are negligible (as is

considered to be the case in this work) or should be properly corrected. The data, thus reduced to the ideal plane-parallel-wall case, may then be considered on a common basis.

EXPERIMENTAL RESULTS

Experimental propane-oxygen-nitrogen quenching data are recorded in table I and curves of critical quenching pressure as a function of oxidant-fuel ratio for four different burner widths and for each of the α values 0.17, 0.21, 0.30, 0.50, 0.70 are shown in figure 5. In these figures, an equivalence ratio scale φ, as well as an oxidant-fuel ratio scale O/F, is given. Stoichiometric oxidant-fuel ratio is indicated in each figure by a short vertical line, placed just above the O/F scale. These curves are entirely analogous to flammability limit curves observed in cylindrical tubes (ref. 5) and are, in fact, flammability limit curves for rectangular channels. The portion of these data relating to propane-air quenching appears to agree quite well with the data reported in reference 4.

As expected, parabola-like curves are obtained, with pressure minima generally located in the region $1.0 < \varphi < 1.2$. The pressure region 0.1 atmosphere to 1.0 atmosphere having been chosen for investigation, it was then necessary to use progressively smaller burner wall separations as α was increased from 0.17 to 0.70. The extent of the data to limiting values of φ on either side of $\varphi = 1$ was essentially determined by either the ability to seat a stable flame on the burner or the pressure range for the investigation. Limit pressure associated with rich flames of cellular structure caused no apparent discontinuity in the variation of p with O/F for any values of α and d investigated.

Data taken from the curves of figure 5 were used to construct least squares logarithmic plots of quenching distance against pressure for each of the five α values investigated and for as wide a range of φ values as the data covered. The slopes of these lines m are related to the observed values of r in table II by the relation

$$m = 2r - 1$$

where

r negative of the power describing the pressure dependence of the quenching distance, $d \propto p^{-r}$

THEORETICAL CONSIDERATIONS

Quenching-Distance Theory

In view of the fact that extensive low-pressure propane-oxygen-nitrogen burning velocity data do not exist, the thermal quenching theory of reference 1 could not be adequately tested. Consequently, only the active-particle quenching-distance equation of reference 2 was examined. This equation is given by

$$d = \left[\frac{A}{k_i} \left(\frac{T_r}{T_0} \right)^n \frac{G}{N_f \sum_i \frac{p_i}{D_i}} \right]^{1/2} \quad (1)$$

where

d quenching distance, cm

A fraction of molecules present in gas phase which must react for flame to continue to propagate

k_i specific rate constant for reaction of active particles of one kind with fuel molecules, $(cm^3)(molecules^{-1})(sec^{-1})$

T_r reaction temperature, ^oK

T_0 initial burner wall temperature and temperature of unburned gas, ^oK

n power describing temperature dependence of diffusion coefficient, $D \propto T^n$

G constant associated with quenching geometry (12 for plane parallel plates)

N_f number of fuel molecules per unit volume, number/cm^3

$\sum_i \frac{p_i}{D_i} = \frac{p_H}{D_H} + \frac{p_{OH}}{D_{OH}} + \frac{p_O}{D_O}$

p_H partial pressure of hydrogen atoms, atm

D_H diffusion coefficient for hydrogen atoms diffusing into unburned gas at 27° C and atmospheric pressure, sq cm/sec

p_{OH} partial pressure of hydroxyl radicals, atm

D_{OH} diffusion coefficient for hydroxyl radicals diffusing into unburned gas at 27° C and atmospheric pressure, sq cm/sec

p_O partial pressure of oxygen atoms, atm

D_O diffusion coefficient for oxygen atoms diffusing into the unburned gas at 27° C and atmospheric pressure, sq cm/sec

The rectangular-slot-burner data of reference 4 were used in reference 2 to test this equation for propane-air flames. The following values were used:

N_f 1/2 of the fuel molecules present in the unburned gas at T_r

n 2

G 12 (for plane parallel plates)

D_H 1.8 sq cm/sec
D_O 0.4 sq cm/sec
D_{OH} 0.28 sq cm/sec
} constant for all compositions
T_r 0.7 T_f

In order to apply equation (1) over a wide range of gas composition, pressure, and temperature, the following conditions should be satisfied:

(1) All the quantities necessary for the calculation of d must be readily obtainable.

(2) Inasmuch as A/k_i is not readily calculable, it should be a known function (preferably a constant) for any given fuel-oxidant system.

(3) Because of the large number of assumptions implicit in the derivation and use of the equation, its correctness and range of applicability should not critically depend upon a very rigid choice of values for those quantities whose true values are open to some debate. Thus, for example, the equation should be useful even when the diffusion coefficients and the temperature dependence of the diffusion coefficients employed are assigned acceptable values other than those used in reference 2.

Calculation of Flame Temperatures, Diffusion Coefficients, and Free Radical Concentrations

In an attempt to correlate the quenching data, as well as to test the usefulness of equation (1), T_f, N_f, p_H, p_O, p_{OH}, D_H, D_O, and D_{OH} were calculated.

The quantities T_f, N_f, p_H, p_O, and p_{OH} were computed by the same methods employed in reference 2. The active particle concentration was obtained from hydrogen atom, oxygen atom, and hydroxyl radical equilibrium product concentrations at flame temperature. The tables of thermodynamic constants of reference 6 and the value of the heat of formation of propane given in reference 7 were used, in conjunction with the matrix method of reference 6 to calculate equilibrium product concentrations and adiabatic flame temperatures. The calculations were made for a range of pressures and oxidant-fuel ratios for each of the propane-oxygen-nitrogen systems investigated. The values of p_i and T_f are given in table III.

In view of the fact that the proper temperature dependences for D_i are uncertain, it was assumed that the temperature dependence of the diffusion coefficients is given by

$$D \propto T^{1.67}$$

The expected range for n is $(3/2 \leq n \leq 2)$. Values of 1.02, 0.29, and 0.26 square centimeters per second were calculated (appendix C) for the diffusion coefficients of hydrogen atoms, oxygen atoms, and hydroxyl radicals, respectively, into a stoichiometric propane-air mixture at a pressure of 1 atmosphere and a temperature of 27° C. The relation suggested by Curtiss and Hirschfelder (ref. 9) was employed to calculate the variation of the diffusion coefficients with composition of the unburned gas. This variation was small. The methods and considerations involved in the calculation of the various diffusion coefficients are given in appendix C.

Pressure Dependence of Quenching Distance

The theory presented in reference 2 predicts the pressure dependence of the quenching distance to be given by

$$d = p^{-\frac{m+1}{2}} = p^{-r} \tag{2}$$

where m is the slope of the straight line defined by

$$\log\left(\frac{p_H}{D_H} + \frac{p_O}{D_O} + \frac{p_{OH}}{D_{OH}}\right) = m \log p + \text{constant} \tag{3}$$

Experimental values of r are obtained from the slope of the least squares logarithmic plot of quenching distance against pressure and are compared to the theoretically predicted ones in table II. This is done for oxidants having α values of 0.17, 0.21, 0.30, 0.50, and 0.70, and for a range of equivalence ratios equal to or less than unity. It should be noted that experimentally and theoretically, r depends on both α and φ. Both theory and experiment show that r tends to increase as α increases and that the value of r does not vary greatly and is close to unity over the range of α values investigated. The average deviation of the theoretical r values from the observed ones is 7.1 percent. The theory predicts that r increases with α and with $\varphi(0 \leq \varphi \leq 1)$. The one calculated exception to this theoretical trend is the case where r varies from 0.88 for $\varphi = 0.94$ to 0.85 for $\varphi = 1.00$ and $\alpha = 0.17$.

This minor inversion may be explained in the following way. The p_{OH} term reaches a maximum at $\varphi < 1.0$ whereas the p_H term reaches a maximum at $\varphi > 1.0$. For $\alpha = 0.17$, the decreasing contribution of $\frac{p_O}{D_O} + \frac{p_{OH}}{D_{OH}}$ outweighs the increasing contribution of p_H/D_H, as φ changes from 0.94 to 1.00. Thus, $\sum_i p_i/D_i$ is smaller at $\varphi = 1.00$ than at $\varphi = 0.94$.

In general, the variation of the observed r values with φ, for a given value of α, is somewhat larger than that predicted by theory. Also, contrary to theory, the observed value of r decreases as φ increases to unity, for values of $\alpha = 0.50$ and 0.70.

It should be noted that expression 2 is derived from a theory which, as expressed in equation (1), is intended for use with lean or stoichiometric mixtures only. The fact that equation (2) does predict a pressure dependence of the quenching distance which agrees well with the observed rich values is shown by the comparison of observed and calculated values of r given in table II. For values of $\varphi > 1$, the average deviation of the calculated r values from the observed ones is 13.6 percent. This relatively good agreement is plausible if it is noted that

(1) Even for the case where $\sum_i p_i/D_i$ becomes quite small, m is not greatly reduced.

(2) The term $p^{-\frac{m+1}{2}}$ was shown to describe the pressure dependence of d as a result of considering all the pressure-dependent terms that appear in equation (1). An equation similar to equation (2) might be possible for rich mixtures if N_f and $\sum_i p_i/D_i$ (eq. (1)) are replaced by other terms having approximately the same pressure dependence.

Comparison of Experimental and Predicted Quenching Distances

Equation (1) has been used successfully (ref. 2) to correlate the propane-air quenching-distance data of reference 4. To test the usefulness of this equation over the range of φ ($\varphi \leq 1$), α, and p encountered in this work, d^2 was plotted against

$$\psi = \left[12 \left(\frac{T_r}{T_O} \right)^{1.67} \frac{1}{N_f \sum_i p_i/D_i} \right]$$

for each value of α. Separate plots for $\alpha = 0.17$, 0.21, 0.30, 0.50, and 0.70 are shown in figure 6. It is seen that a good straight-line plot is defined in each case, indicating

$$\frac{A}{k_i} = \frac{d^2}{\dfrac{12\ (T_r/T_0)^{1.67}}{N_f \sum_i p_i/D_i}} = \frac{d^2}{\psi}$$

is equal to a constant for each value of α. From the slopes of the d^2 against ψ plots (fig. 6) it is found that A/k_i increases from a value of 0.1694×10^{12} molecule-seconds per cubic centimeter, for $\alpha = 0.17$, to a value of 0.2360×10^{12} for $\alpha = 0.70$. It should be noted that the percent deviation of the observed values of d from those which may be predicted is only one half as large as the corresponding percent deviations indicated for d^2.

Although the dependence of A/k_i on α is too large to be neglected, it may be observed from figure 7 that a logarithmic plot of d^2 against ψ (which includes the data for all observed values of α and for $\varphi \leq 1$) correlates the data quite nicely. A semilogarithmic plot of A/k_i against α is shown in figure 8. If it is assumed that A is constant for all α, then one is led to the conclusion that k_i decreases with α (or T). This could be possible only if the reaction mechanism were changing in just the right way. But then the validity of assumptions concerning the nature of the over-all reaction is greatly weakened. The specific rate constant has been calculated from burning-velocity data according to the method employed in reference 9 and a plot of k_i against α is shown in figure 9. As expected, k_i increases with increasing α. That A is not a true constant is suggested by the fact that both A/k_i and k_i increase with α, even when calculations are made by the methods of reference 2. From this treatment it appears that the quenching distance equation term A/k_i is a proportionality factor that is very mildly dependent upon α. When so considered, equation (1) was found to predict propane-oxygen-nitrogen system quenching distances within 4.2 percent of the experimental values for a range of α and p values for values of $\varphi \leq 1$. This 4.2 percent deviation represents an average value for the 64 quenching-distance values used in constructing the curves of figure 6. The fact that it is a relatively small deviation strongly supports the main premise of reference 2, namely that $d^2 \varpropto \psi$. This good agreement has been obtained even when the temperature dependence of the diffusion coefficients was changed from $n = 2.00$ to $n = 1.67$ and when other reasonable values for D_{OH}, D_H, and D_O were substituted for those employed in reference 2.

As noted earlier, equation (1) cannot be expected to be valid for values of $\varphi > 1$. However, if equation (1) is applied to data of rich mixtures, it is found that the equation represents the data very badly for low values of α but that it improves markedly as α increases to 0.70. This can be used, perhaps, as a measure of how different the over-all rich side kinetics are from those on the lean side.

It should be further noted that the success of equation (1) in no way rules out the possibility that a thermal theory of flame quenching could be made to work as well.

SUMMARY OF RESULTS

The results of an investigation of flame quenching by a variable-width rectangular-slot burner as a function of pressure for various propane-oxygen-nitrogen mixtures may be summarized as follows:

1. Critical quenching pressure against oxidant-fuel ratio curves have been obtained. Pressures between 0.1 atmosphere and 1.0 atmosphere as well as four burner widths for each of the oxygen fraction $O_2/(O_2 + N_2)$ values 0.17, 0.21, 0.30, 0.50, and 0.70 were investigated.

2. Calculations have been made and curves presented which give the error incurred in assuming that flame quenching by rectangular channels is equivalent to flame quenching by plane parallel plates of infinite extent. The error inherent in this assumption is related to the length-to-width ratio of the rectangular burner.

3. For equivalence ratios φ approximately equal to unity, the observed relation between pressure p and quenching distance d ($d \propto p^{-r}$) is approximately given by $r = 1$. For the range of $O_2/(O_2 + N_2)$ and φ values investigated, $0.60 \leq r \leq 1.12$.

4. Calculations made by the quenching-distance equation proposed by Simon and Belles predict a pressure dependence of the quenching distance which deviates from the observed pressure dependence by an average of 7.1 percent for $\varphi \leq 1$ and by an average of 13.6 percent for $\varphi > 1$.

5. Application of this quenching-distance equation to the data indicates that:

   (a) The variation of the square of the quenching distance with ψ, for a given value of $O_2/(O_2 + N_2)$ and for values of $\varphi \leq 1$, is preserved even when the value of n (the temperature dependence of the diffusion coefficient) is changed from 2 to 1.67 and when values for D_1 significantly different from those originally used by Simon and Belles are employed.

$$d^2 \propto \psi = \frac{12\ (T_r/T_0)^n}{N_f \sum_i p_i/D_i}$$

(where T_r and T_0 are the temperatures of the reaction and the cold gas, respectively, N_f is the number of fuel molecules per unit volume, and p_i and D_i are the partial pressure and the diffusion coefficient, respectively, for the i^{th} species)

(b) The quenching equation may be used to predict the quenching distances for values of $\varphi \leq 1$. These predicted values deviate from the observed ones by an average of 4.2 percent.

(c) For values of $\varphi > 1$ and in its present form, the quenching equation cannot properly be used to predict the observed quenching distances.

CONCLUSIONS

From the results of this investigation it may be concluded that:

1. The quenching distance as measured by plane parallel plates of infinite extent differs by less than 3 percent from that obtained through use of a rectangular burner, as long as the length-to-width ratio of the rectangular burner is 10 or greater.

2. The pressure dependence of the quenching distance does not vary appreciably with oxygen concentration of the oxidants.

3. An equation based on diffusion processes may be successfully used to predict propane-oxygen-nitrogen quenching distances for a range of pressures, fuel-oxidant ratios, and oxygen concentrations of the oxidant, for values of $\varphi \leq 1$.

Lewis Flight Propulsion Laboratory
National Advisory Committee for Aeronautics
Cleveland, Ohio, November 25, 1953

APPENDIX A

SYMBOLS

The following symbols are used in this report:

A	fraction of molecules present in the gas phase which must react for the flame to continue to propagate
b	length of rectangular burner lip
C_T	total number of active particles in rectangular channel
c	numerical concentration of active particles
$\bar{c}$	average concentration of active particles per unit volume
c_0	number of active particles generated per unit time per unit volume
D_H	diffusion coefficient associated with diffusion of hydrogen atoms into unburned gas at 27° C and p = 1 atmosphere
D_{ij}	diffusion coefficient associated with mixture of two gases of species i and j
D_O	diffusion coefficient associated with diffusion of oxygen atoms into unburned gas at 27° C and p = 1 atmosphere
D_{OH}	diffusion coefficient associated with diffusion of hydroxyl radicals into unburned gas at 27° C and p = 1 atmosphere
d	quenching distance
d_c	diameter of cylindrical burner that will just quench a given flame
d_p	wall separation of plane parallel wall burner that will just quench a given flame
d_r	width of rectangular burner that will just quench a given flame
G	constant associated with quenching geometry
k	Boltzmann constant (c.g.s. units)
k_i	specific rate constant for reaction of active particles of one kind with fuel molecules

m_i mass of molecule of species i

N number density of molecules

N_f number of fuel molecules per unit volume

n power describing temperature dependence of diffusion coefficient, $D \propto T^n$

O/F oxidant-fuel mass ratio

$(O/F)_S$ stoichiometric oxidant-fuel mass ratio

p total pressure

p_H partial pressure of hydrogen atoms

p_i partial pressure of i^{th} molecular species

p_O partial pressure of oxygen atoms

p_{OH} partial pressure of hydroxyl radicals

r negative of power describing pressure dependence of quenching distance, $d \propto p^{-r}$

r_i molecular radius for particle of species i

T_f flame temperature

T_r reaction temperature

T_O cold gas temperature

α $O_2/(O_2 + N_2)$, volumetric ratio of oxygen content of oxidant to oxygen content of air

μ viscosity

$$\sum_i \frac{p_i}{D_i} = \frac{p_H}{D_H} + \frac{p_{OH}}{D_{OH}} + \frac{p_O}{D_O}$$

φ equivalence ratio $= (O/F)_S/(O/F)$

$$\psi = \frac{12\ (T_r/T_O)^n}{N_f \sum_i p_i/D_i}$$

APPENDIX B

QUENCHING EFFECTS OF RECTANGULAR CHANNELS COMPARED TO THOSE OBTAINED FOR PLANE PARALLEL PLATES OF INFINITE EXTENT

Consider a rectangle with center at the origin of the xy-plane. The rectangle is of length b and of width d. Let this rectangle correspond to a typical cross section of a rectangular channel of infinite extent, in which active particles are being generated uniformly throughout the volume. It is assumed that all active species are destroyed on collision with the walls.

The differential equation of diffusion describing this case is

$$\frac{\partial^2 c}{\partial x^2} + \frac{\partial^2 c}{\partial y^2} = -\frac{c_0}{D} \tag{B1}$$

subject to the boundary conditions

$$c = 0 \quad \text{at} \quad \left\{ \begin{array}{l} x = \pm d/2 \\ y = y \end{array} \right\}$$

and

$$c = 0 \quad \text{at} \quad \left\{ \begin{array}{l} x = x \\ y = \pm b/2 \end{array} \right\}$$

where

c numerical concentration of active particles

c_0 number of particles generated per unit time per unit volume

D diffusion coefficient

Considering a unit height, the total number of active particles in the rectangular channel C_T is given by

$$C_T = 4 \int_0^{b/2} \int_0^{d/2} c \, dx \, dy = 4 \bar{c} \int_0^{b/2} \int_0^{d/2} dx \, dy = \bar{c} \, bd \tag{B3}$$

where

$\bar{c}$ average concentration of active particles in volume

The formal mathematical problem associated with equation (B1) and its accompanying boundary conditions (B2) corresponds to other physical problems which have already been treated and are presented by Jakob and by Purday (refs. 10 and 11, respectively). The results obtained by these authors for various rectangular geometries may be employed to calculate $\bar{c}$ and thus to construct the curves of figures 4 and 5.

It is significant to note that the formal mathematical problem is unchanged if the previously stated diffusion problem is replaced by one in which heat is being generated uniformly in the volume and lost to walls of a given temperature. The very same effect of geometry on quenching distance is predicted on the basis of this thermal calculation, if it is assumed that flame propagation or nonpropagation is determined by some critical value of the average flame temperature.

APPENDIX C

DIFFUSION COEFFICIENT CALCULATIONS

The molecular and atomic radii employed in the diffusion coefficient calculations were obtained from several sources. For a pressure of 1 atmosphere and a temperature of 0° C,

(1) $r_O = 1.40 \times 10^{-8}$ centimeter is the value for the atomic oxygen radius given by Pauling (ref. 12).

(2) $r_{O_2} = 1.81 \times 10^{-8}$ centimeter is the value for the radius of the oxygen molecules given by Chapman and Cowling (ref. 13).

(3) $r_{N_2} = 1.88 \times 10^{-8}$ centimeter is the value for the radius of the nitrogen molecule given in reference 13.

(4) $r_H = 1.28 \times 10^{-8}$ centimeter is the value for the atomic hydrogen radius calculated from the viscosity data given by Amdur (ref. 14). This calculation was made with the following equation (ref. 13):

$$\mu = \frac{0.1792\ (km_i T)^{1/2}}{4 r_i^{\,2}}$$

where all units are of the c.g.s. system and where

μ viscosity

k Boltzmann's constant

m_i molecular mass

T absolute temperature

r_i molecular radius

(5) $r_{OH} = 1.62 \times 10^{-8}$ centimeter is the radius of the hydroxyl radical and represents a weighted average of the values obtained from

$$r_{OH} = \frac{1}{2}\ (r_{H_2} + r_{O_2})$$

and

$$r_{OH} = \left[(r_H)^3 + (r_O)^3 \right]^{1/3}$$

where

r_{H_2} 1.365×10^{-8} centimeter (ref. 14)

(6) $r_{C_3H_8} = 3.11 \times 10^{-8}$ centimeter is the radius of the propane molecule, calculated from the viscosity data of reference 15.

The diffusion coefficient for a mixture of any two gases was calculated from the equation (ref. 13)

$$D_{ij} = \frac{3}{8N (r_i + r_j)^2} \left[\frac{kT (m_i + m_j)}{2\pi m_i m_j} \right]^{1/2} \qquad (C1)$$

where

N number density of molecules

i,j subscripts identifying the molecular species

Examination of the table on page 252 of reference 13 indicates that, for the binary mixtures listed, use of the r values determined from viscosity data does not yield, on the average, the experimentally determined values of D_{ij}. In fact, the r values that do yield the experimentally determined values of D_{ij} (eq. (C1)) are, on the average, equal to 91.7 percent of the r values determined from viscosity measurements. Consequently, the r values used in equation (C1) were appropriately adjusted. For a pressure of 1 atmosphere and a temperature of 300° K, the following values of D_{ij} were obtained. Units of D_{ij} are square centimeters per second.

$D_{H\text{-}C_3H_8} = 0.547$	$D_{O\text{-}C_3H_8} = 0.149$	$D_{OH\text{-}C_3H_8} = 0.143$
$D_{H\text{-}O_2} = 1.11$	$D_{O\text{-}O_2} = 0.311$	$D_{OH\text{-}O_2} = 0.266$
$D_{H\text{-}N_2} = 1.06$	$D_{O\text{-}N_2} = 0.304$	$D_{OH\text{-}N_2} = 0.262$

It was then assumed that the reciprocal of the average diffusion coefficient for a multicomponent gas mixture is given by the molal average of the reciprocals of the binary coefficients. This method, suggested by Curtiss and Hirschfelder (ref. 8), was then used to calculate the diffusion coefficients for the diffusion of O, H, and OH into the various O_2 - N_2 - C_3H_8 mixtures encountered.

REFERENCES

1. Lewis, Bernard, and von Elbe, Guenther: Combustion, Flames, and Explosions of Gases. Academic Press, Inc. (New York), 1951.

2. Simon, Dorothy M., Belles, Frank E., and Sapkowski, Adolph E.: Investigation and Interpretation of the Flammability Region for Some Lean Hydrocarbon-Air Mixtures. Fourth Symposium (International), on Combustion. The Williams & Wilkins Co., 1953, pp. 126-138.

3. Semenoff, N.: Chemical Kinetics and Chain Reactions. Clarendon Press (Oxford), 1935.

4. Friedman, Raymond, and Johnston, W. C.: The Wall-Quenching of Laminar Flames as a Function of Pressure, Temperature, and Air-Fuel Ratio. Jour. Appl. Phys., vol. 21, no. 8, Aug. 1950, pp. 791-795.

5. Belles, Frank E., and Simon, Dorothy M.: Variation of the Pressure Limits of Flame Propagation with Tube Diameter for Propane-Air Mixtures. NACA RM E51J09, 1951.

6. Huff, Vearl N., Gordon, Sanford, and Morrell, Virginia E.: General Method and Thermodynamic Tables for Computation of Equilibrium Composition and Temperature of Chemical Reactions. NACA Rep. 1037, 1951. (Supersedes NACA TN's 2113 and 2161.)

7. Rossini, Frederick D., et al.: Selected Values of Properties of Hydrocarbons. Circular C461, Nat. Bur. Standards, Nov. 1947.

8. Curtiss, Charles F., and Hirschfelder, Joseph O.: Transport Properties of Multicomponent Gas Mixtures. Jour. Chem. Phys., vol. 17, no. 6, June 1949, pp. 550-555.

9. Dugger, Gordon L., and Simon, Dorothy M.: Prediction of Flame Velocities of Hydrocarbon Flames. NACA RM E52J13, 1952.

10. Jakob, Max: Heat Transfer. Vol. 1. John Wiley & Sons, Inc., 1949, pp. 177-180.

11. Purday, H. F. P.: An Introduction to the Mechanics of Viscous Flow. Dover Pub., Inc., 1949, pp. 16-18.

12. Pauling, Linus: The Nature of the Chemical Bond. Second ed., Cornell Univ. Press, 1940, p. 189.

13. Chapman, Sydney, and Cowling, T. G.: The Mathematical Theory of Non-Uniform Gases. Cambridge Univ. Press (Cambridge, England), 1939.

14. Amdur, I.: Viscosity and Diffusion Coefficients of Atomic Hydrogen and Atomic Deuterium. Jour. Chem. Phys., vol. 4, no. 6, June 1936, pp. 339-343.

15. Perry, John H., ed.: Chemical Engineers' Handbook. Third ed., McGraw-Hill Book Co., Inc., 1950.

TABLE I. - OBSERVED QUENCHING DATA

Quenching distance, d, in.	Oxidant-fuel mass ratio, O/F	Pressure, p, in. Hg	Fuel-oxidant mass ratio, F/O	Quenching distance, d, in.	Oxidant-fuel mass ratio, O/F	Pressure, p, in. Hg	Fuel-oxidant mass ratio, F/O
Oxygen fraction, α, 0.17							
0.215	12.74	19.5	0.07849	0.375	15.26	7.60	0.06553
	13.38	17.1	.07474		16.16	7.85	.06188
	15.4	14.8	.06494		17.31	8.80	.05777
	16.32	15.5	.06127		17.92	9.50	.05580
	17.60	17.1	.05682		19.57	11.90	.05110
	18.56	18.7	.05388		13.58	7.75	.07364
	19.81	22.05	.06048		20.21	12.95	.04948
	19.00	19.25	.05263		12.90	8.30	.07752
	12.25	21.15	.08163		12.22	9.25	.08183
	12.21	23.60	.08190		11.83	10.90	.08453
	16.55	15.98	.06042		11.44	12.60	.08741
	20.60	26.2	.04854		11.42	16.20	.08757
0.300	17.91	12.2	0.05583	0.500	11.26	22.45	0.09560
	16.77	11.0	.05965		11.30	14.02	.09533
	15.68	10.7	.06388		11.33	11.32	.09320
	14.30	11.2	.06993		11.45	10.88	.09217
	19.29	14.1	.05184		11.55	9.70	.09050
	20.29	16.3	.04929		11.75	8.90	.08689
	20.78	17.8	.04812		11.94	7.90	.08591
	13.65	12.0	.07326		12.06	7.07	.08292
	12.70	14.0	.07874		12.82	6.52	.07924
	11.89	18.4	.08410		13.45	6.02	.07435
	12.29	16.1	.08157		15.58	5.72	.06418
	11.80	22.9	.08475		17.35	6.20	.05764
					18.52	7.01	.05400
					19.34	7.82	.05171
					20.36	9.44	.04911
Oxygen fraction, α, 0.21							
0.150	10.52	28.43	0.09506	0.300	9.81	28.52	0.1019
	10.74	25.51	.09311		9.83	22.06	.1017
	11.46	18.15	.08726		9.98	16.67	.1002
	13.03	14.70	.07675		10.84	11.71	.09338
	14.51	13.88	.06892		11.05	10.22	.09056
	16.52	14.81	.06053		11.69	8.48	.08554
	19.03	18.62	.05255		13.14	6.57	.07610
	20.96	24.36	.04771		14.26	5.93	.07015
	21.90	27.73	.04568		15.68	6.21	.06398
					19.01	8.27	.05260
					18.38	7.78	.06438
					21.03	11.64	.04755
					22.32	15.93	.04480
					23.18	20.55	.04318
					23.67	24.87	.04225
					23.86	27.94	.04188
0.200	10.28	25.24	0.09728	0.500	8.22	27.85	0.1050
	10.61	19.63	.09425		8.44	24.14	.1048
	11.46	14.62	.08726		8.80	18.83	.1042
	13.12	11.18	.07622		9.24	13.18	.1016
	14.69	9.96	.06807		10.10	8.56	.09524
	15.88	10.14	.06297		11.23	8.02	.08905
	17.07	10.93	.05858		12.81	4.31	.07806
	18.51	12.68	.05402		14.48	3.56	.06906
	20.23	16.25	.04943		16.78	3.60	.05957
	21.56	20.64	.04634		18.69	4.12	.05350
	22.17	23.58	.04511		20.18	5.39	.04955
	22.86	28.17	.04374		22.45	8.67	.04456
					24.16	14.93	.04139
					24.52	20.06	.04078
					24.63	24.37	.04060
					24.71	26.89	.04047
Oxygen fraction, α, 0.30							
0.100	19.60	28.72	0.05102	0.215	14.26	5.53	0.07013
	18.92	24.88	.05285		15.98	6.55	.06258
	17.80	20.16	.05618		19.07	9.33	.05244
	15.48	12.75	.06460		11.18	4.61	.08945
	13.10	10.78	.07634		9.127	4.70	.1096
	11.84	10.26	.08446		9.535	4.56	.1049
	10.98	10.22	.09107		8.432	5.11	.1186
	9.27	10.90	.1079		18.48	8.33	.05411
	7.42	12.38	.1348		21.33	14.86	.04688
	6.68	15.10	.1497		23.05	20.77	.04338
	6.41	18.78	.1560		23.89	25.28	.04186
	5.75	25.20	.1739		23.96	29.10	.04174
	5.61	28.52	.1783		4.590	28.50	.2179
					4.673	25.25	.2140
					4.910	18.26	.2037
					5.096	14.62	.1962
					5.772	9.98	.1733
					6.582	7.12	.1519
					7.247	6.49	.1380
					8.038	5.11	.1244
0.175	4.771	27.92	0.2096	0.300	4.11	28.15	0.2433
	4.939	23.18	.2025		4.20	24.2	.2381
	5.197	18.88	.1924		4.37	18.26	.2288
	5.822	11.81	.1718		4.77	10.45	.2098
	6.714	8.63	.1489		5.31	6.96	.1883
	18.42	11.83	.05429		5.46	6.22	.1832
	20.47	16.21	.04885		6.506	5.15	.1537
	22.36	21.92	.04472		7.116	4.12	.1406
	23.83	29.05	.04196		7.824	3.58	.1278
	9.78	5.82	.1022		8.591	3.27	.1164
	14.03	6.04	.07128		9.469	3.22	.1056
					10.12	3.26	.09881
					10.98	3.43	.08107
					11.92	3.81	.08389
					14.65	4.22	.06826
					17.78	5.38	.05624
					19.28	6.48	.05187
					22.15	10.04	.04515
					24.40	16.11	.04098
					25.62	24.33	.03903

TABLE I. - Concluded. OBSERVED QUENCHING DATA

Quenching distance, d, in.	Oxidant-fuel mass ratio, O/F	Pressure, p, in. Hg	Fuel-oxidant mass ratio, F/O	Quenching distance, d, in.	Oxidant-fuel mass ratio, O/F	Pressure, p, in. Hg	Fuel-oxidant mass ratio, F/O
Oxygen fraction, α, 0.50							
0.040	6.715	13.95	0.1489	0.100	5.478	5.26	0.1825
	7.444	14.40	.1343		4.953	5.57	.2019
	8.316	15.22	.1203		4.419	6.68	.2263
	10.92	18.82	.09158		4.019	7.65	.2488
	12.11	21.63	.08258		3.288	12.33	.3041
	14.51	28.2	.06892		3.047	15.15	.3282
	7.142	13.96	.1400		2.848	19.53	.3511
	5.799	13.71	.1724		2.694	24.65	.3712
	4.817	14.86	.2076		6.352	5.25	.1574
	4.001	19.72	.2499		7.222	5.28	.1385
	3.729	22.85	.2682		7.951	5.48	.1258
	3.435	25.78	.2911		9.469	6.03	.1056
					11.48	7.41	0.08711
					12.58	8.50	.07949
					16.11	14.20	.06207
					18.17	19.34	.05504
					19.39	24.68	.05157
					19.76	28.64	.05061
0.075	6.413	7.16	0.1559	0.125	5.892	4.33	0.1697
	7.47	7.46	.1339		7.638	4.74	.1309
	9.526	8.73	.1050		6.679	4.43	.1497
	11.78	10.73	.08489		4.835	4.45	.2068
	14.74	15.54	.06784		4.024	5.19	.2485
	16.99	21.67	.05886		9.080	5.37	.1101
	17.91	25.29	.05583		11.23	6.84	.08905
	18.35	28.00	.05450		14.61	9.86	.06845
	5.036	7.52	.1986		16.38	15.16	.06105
	4.056	9.91	.2465		18.00	17.57	.05556
	3.457	13.96	.2893		19.06	23.45	.05247
	3.049	20.2	.3280		19.55	27.55	.05115
	2.893	23.9	.3457		3.50	7.15	.2857
	2.862	26.65	.3494		3.19	11.25	.3135
Oxygen fraction, α, 0.70							
0.040	5.923	9.83	0.1688	0.075	5.184	5.27	0.1929
	4.851	9.26	.2061		6.583	5.86	.1519
	4.094	9.26	.2443		7.909	6.65	.1264
	3.547	9.83	.2819		10.12	8.04	.09881
	7.931	11.59	.1261		11.50	9.39	.08696
	9.099	13.19	.1099		13.61	12.21	.07348
	10.55	16.06	.09479		15.58	16.29	.06418
	12.87	20.63	.07770		2.155	26.30	.4640
	14.34	26.29	.06974		2.227	21.55	.4490
	2.682	27.15	.3729		2.364	17.16	.4230
	2.792	21.60	.3582		2.605	13.27	.3839
	3.270	16.30	.3058		3.043	8.59	.3286
					3.370	7.69	.2967
					3.794	6.23	.2636
0.050	5.911	7.73	0.1692	0.100	2.274	14.15	0.4398
	6.834	8.39	.1463		2.628	9.02	.3805
	4.671	7.45	.2141		2.063	20.10	.4847
	4.127	7.41	.2423		1.954	26.10	.5118
	3.525	7.86	.2837		16.85	20.81	.05935
	8.307	9.59	.1204		17.46	26.16	.05727
	9.763	11.28	.1024		12.07	8.48	.08285
	11.10	13.61	.09009		15.06	13.87	.06640
	13.58	17.61	.07364		9.087	5.09	.1100
	14.84	21.61	.06739		4.302	3.74	.2325
	15.96	25.68	.06266		3.269	4.60	.3059
	16.85	28.55	.05935		2.647	6.41	.3778
	1.940	27.60	.5155		4.873	3.71	.2052
	2.051	22.60	.4876		5.855	3.83	.1708
	2.277	16.65	.4392		7.008	4.16	.1427
	2.638	12.16	.3791				
	2.973	9.78	.3364				

TABLE II. - COMPARISON OF PREDICTED AND OBSERVED PRESSURE DEPENDENCE OF QUENCHING DISTANCE

Oxygen fraction, α	Equivalence ratio, φ	Pressure dependence of quenching distance, r	
		Observed	Predicted
0.17	0.943	0.90	0.88
	1.000	.89	.85
	1.340	.84	.75
	1.530	.71	.75
0.21	0.738	0.85	0.86
	.864	.84	.89
	1.000	.89	.93
	1.240	.95	.78
	1.490	.98	.76
0.30	0.566	0.76	0.87
	.662	.93	.89
	.773	1.06	.92
	1.000	.98	.94
	1.380	.93	.86
	1.903	.74	.76
0.50	0.476	1.01	0.91
	.544	1.01	.93
	.680	.96	.96
	1.000	.93	.97
	1.358	.91	.95
	1.940	.88	.82
0.70	0.345	1.12	0.91
	.395	1.12	.93
	.494	1.02	.96
	1.000	1.01	.98
	1.234	1.07	.98
	1.829	.60	.89

TABLE III. - EQUILIBRIUM FLAME TEMPERATURES AND ACTIVE PARTICLE CONCENTRATIONS FOR $\varphi \leq 1$

Equivalence ratio, φ	Pressure, p, atm	Flame temperature, T_f, °K	Partial pressures, atm		
			P_{OH}	P_H	P_O
$\alpha = 0.17$					
1.000	0.6584	2045	0.511×10^{-3}	0.0717×10^{-3}	0.0317×10^{-3}
	.4595	2039	.398	.0600	.0275
	.3720	2037	.340	.0543	.0251
	.2530	2032	.257	.0453	.0215
$\alpha = 0.21$					
1.000	0.4719	2219	1.52×10^{-3}	0.311×10^{-3}	0.227×10^{-3}
	.3352	2214	1.13	.255	.182
	.2075	2208	.748	.190	.155
	.1160	2200	.462	.134	.0937
.884	.5551	2126	1.37	.0760	.215
	.4027	2120	1.05	.0655	.177
	.2510	2112	.710	.0627	.142
	.1283	2100	.414	.0389	.0883
.738	.8388	1940	.844	.0947	.116
	.6353	1939	.680	.0885	.0974
	.3970	1937	.485	.0748	.0735
	.2186	1934	.308	.0609	.0510
$\alpha = 0.30$					
1.000	0.3419	2495	4.334×10^{-3}	1.606×10^{-3}	1.321×10^{-3}
	.1872	2459	2.479	1.051	.845
	.1521	2446	2.070	.900	.718
	.1133	2429	1.549	.753	.577
.7726	.3786	2353	3.484	.419	1.121
	.2079	2331	2.040	.298	.729
	.1848	2325	1.840	.279	.669
	.1343	2313	1.578	.232	.537
.6623	.5297	2215	2.759	.127	.707
	.2871	2202	1.640	.0968	.481
	.2546	2198	1.390	.0885	.424
	.1611	2190	1.012	.0756	.338
.5862	.9451	2035	1.922	.0237	.322
	.4615	2031	1.100	.0189	.218
	.3589	2029	.901	.0173	.189
	.2189	2026	.812	.0149	.145

Equivalence ratio, φ	Pressure, p, atm	Flame temperature, T_f, °K	Partial pressures, atm		
			P_{OH}	P_H	P_O
$\alpha = 0.50$					
1.000	0.4659	2776	17.21×10^{-3}	9.11×10^{-3}	8.08×10^{-3}
	.2420	2716	8.97	5.39	4.64
	.1758	2687	6.53	4.19	3.55
	.1477	2671	5.47	3.61	3.05
.6798	.5648	2851	16.70	3.33	8.63
	.3028	2808	9.10	2.12	5.13
	.2115	2580	6.42	1.64	3.85
	.1932	2573	5.90	1.54	3.58
.5438	.7176	2519	13.84	1.31	6.35
	.3897	2488	7.87	.901	4.00
	.2824	2472	5.82	.739	3.13
	.2583	2467	5.39	.701	2.95
.4759	.9090	2412	11.60	.601	4.52
	.4853	2390	6.67	.434	2.93
	.3606	2380	5.13	.372	2.40
	.3235	2378	4.68	.352	2.22
$\alpha = 0.70$					
1.000	0.3118	2852	17.98×10^{-3}	11.99×10^{-3}	10.68×10^{-3}
	.2480	2827	14.22	9.89	8.70
	.1765	2792	9.95	7.39	6.38
	.1240	2755	6.99	5.49	4.68
.4938	.4876	2665	18.76	2.96	12.13
	.3890	2648	14.90	2.48	9.95
	.2680	2620	10.40	1.90	7.32
	.1965	2597	7.72	1.53	5.89
.3951	.6584	2528	15.65	1.169	8.61
	.5163	2515	12.50	1.001	7.19
	.3535	2495	8.83	.787	5.34
	.2948	2485	7.43	.713	4.68
.3452	.8689	2424	13.57	.569	6.24
	.6557	2414	10.50	.487	5.09
	.4556	2401	7.61	.405	3.93
	.3914	2395	6.71	.375	3.58

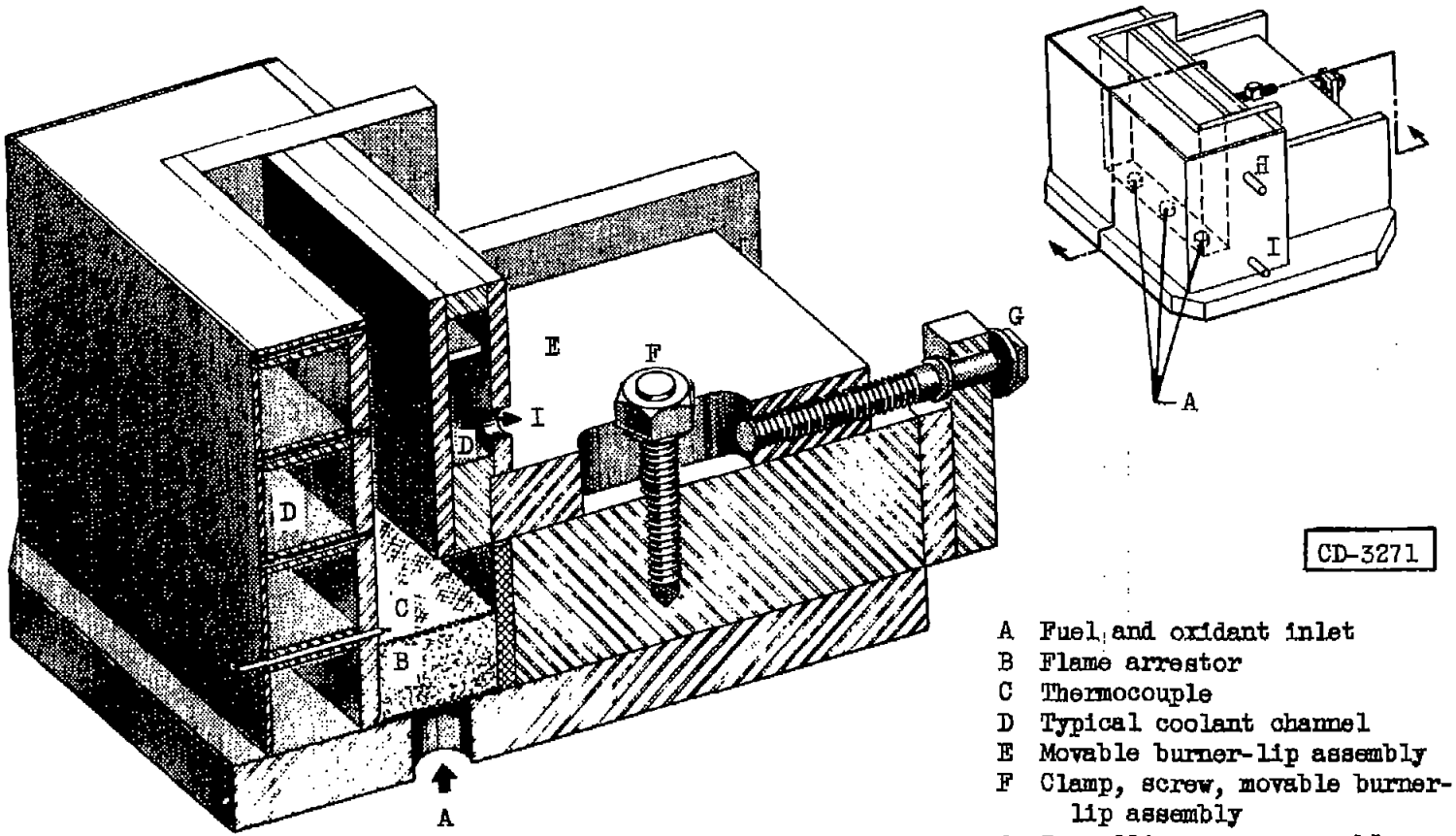

A Fuel and oxidant inlet
B Flame arrestor
C Thermocouple
D Typical coolant channel
E Movable burner-lip assembly
F Clamp, screw, movable burner-lip assembly
G Propelling screw, movable burner-lip assembly
H Coolant inlet
I Coolant outlet

Figure 1. - Quenching distance burner.

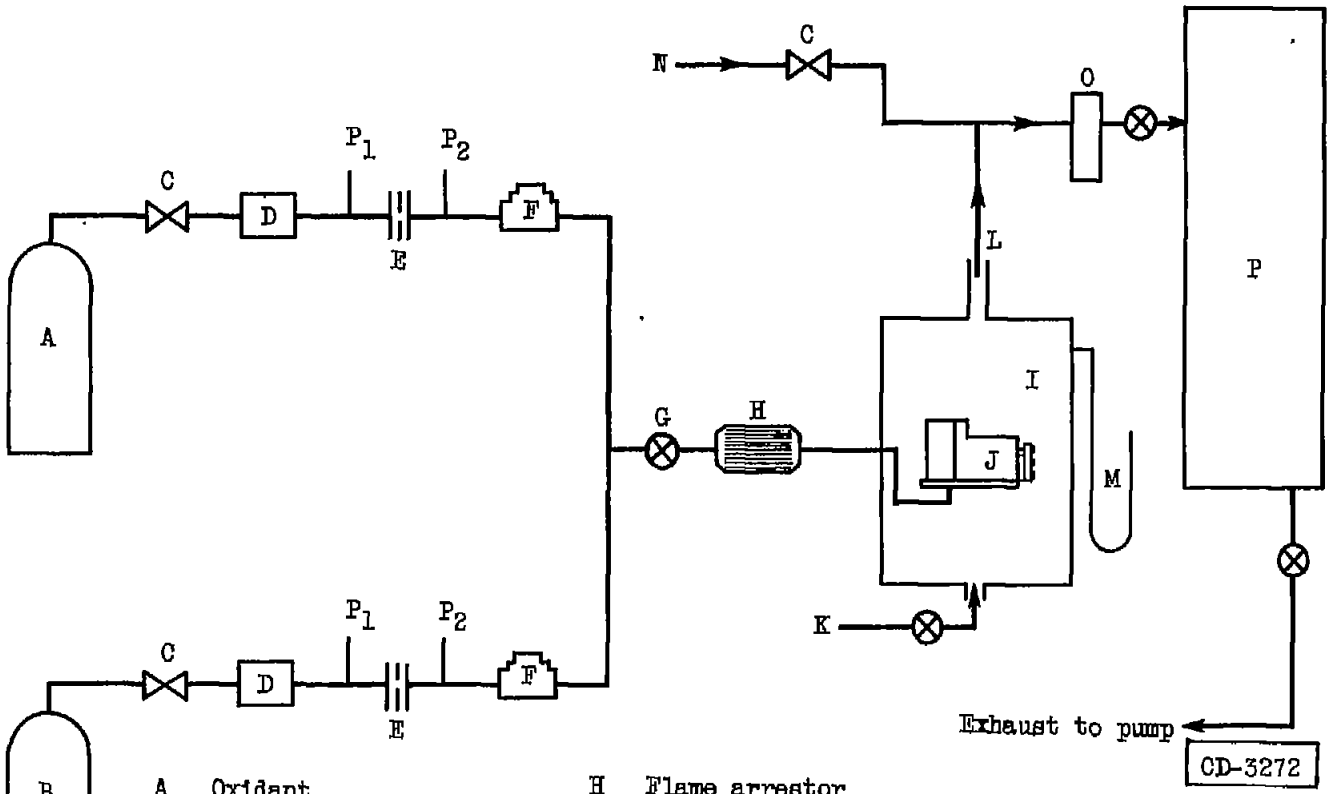

A	Oxidant	H	Flame arrestor
B	Fuel	I	Burner chamber
C	Pressure regulator	J	Burner
D	Filter	K	Room air or nitrogen bleed
P_1	Pressure gage, upstream	L	Burner chamber exhaust
P_2	Pressure gage, downstream	M	Manometer
E	Critical-flow orifice	N	Service air feed to exhaust
F	Solenoid valve	O	Cold trap
G	Valve	P	Plenum

Figure 2. - Schematic flow diagram.

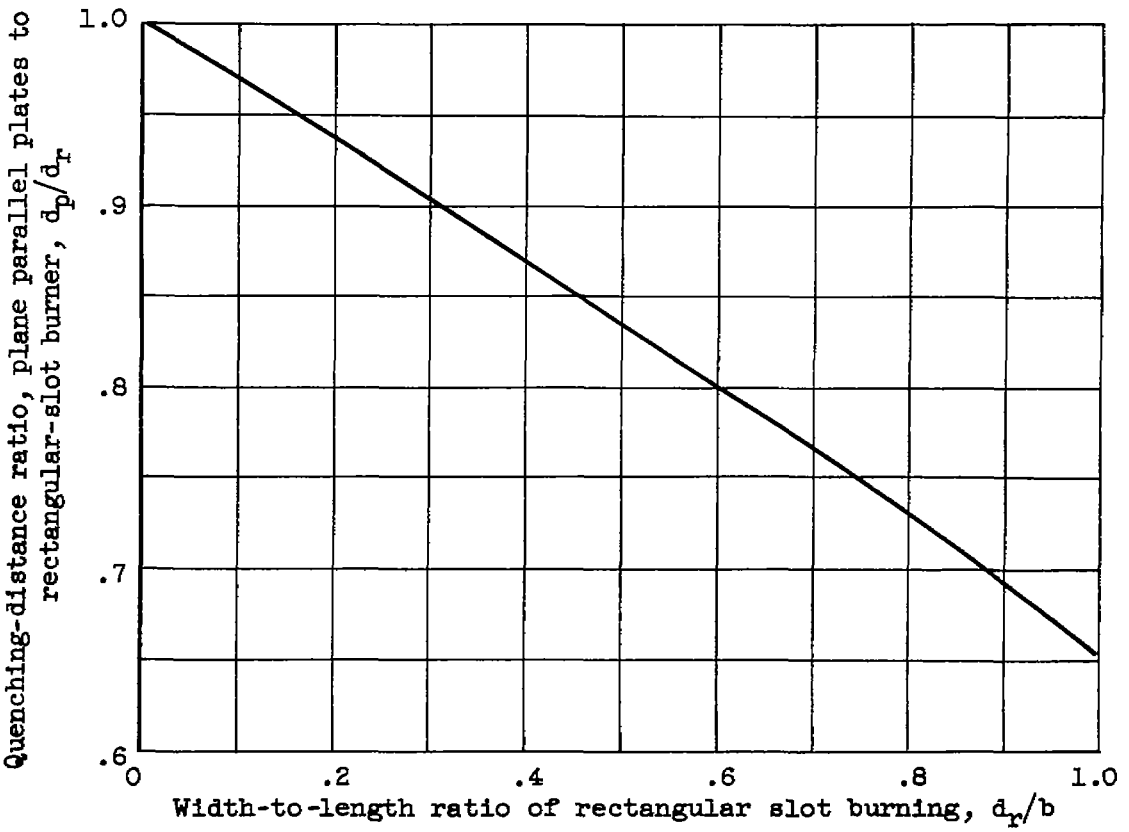

Figure 3. - Calculated rectangular-slot-burner quenching distances compared with plane-parallel-burner quenching distances as a function of width-to-length ratio of rectangular burner.

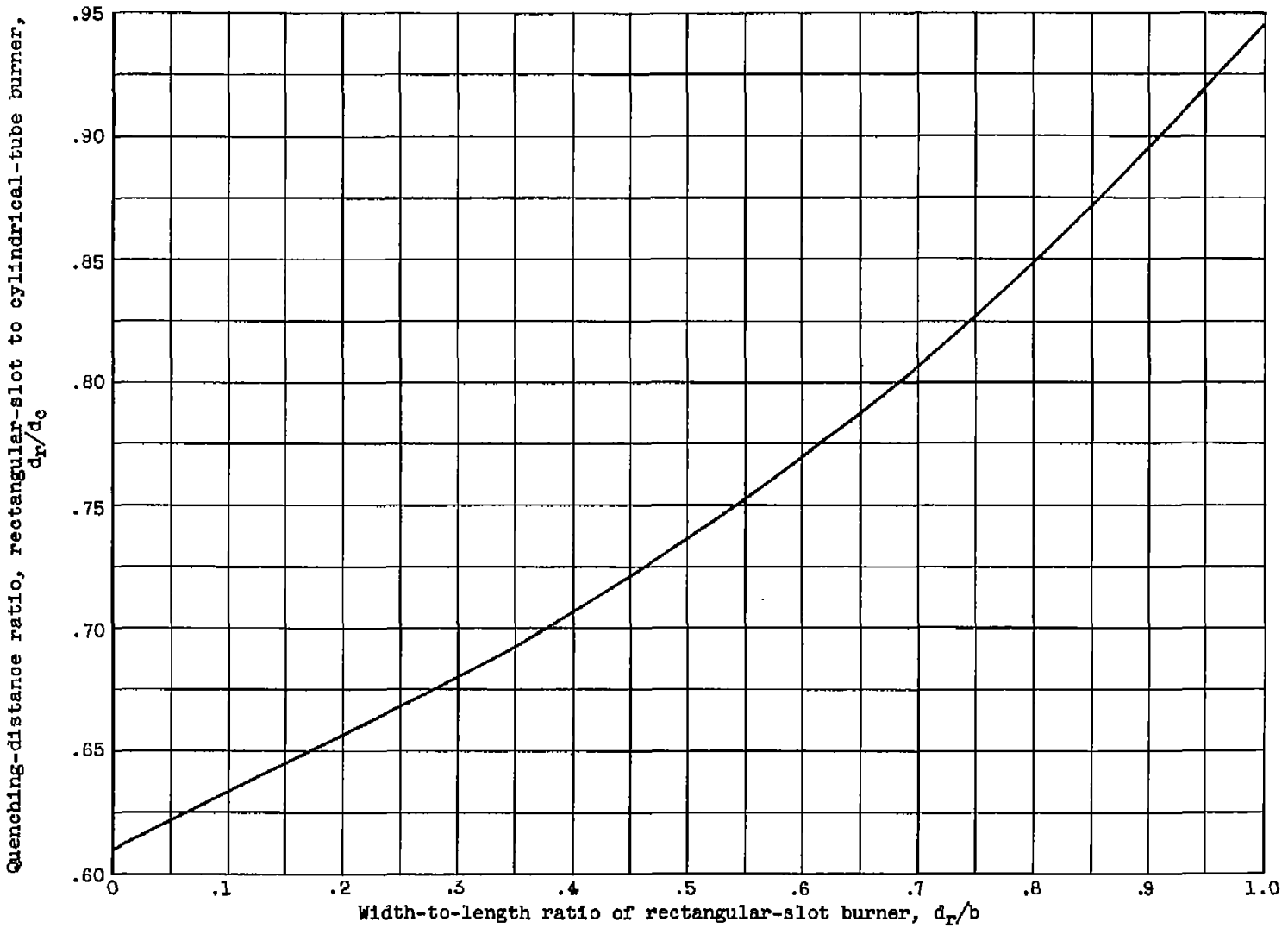

Figure 4. - Calculated rectangular-slot-burner quenching distances compared with cylindrical-burner quenching diameters as function of width-to-length ratio of rectangular-slot burner.

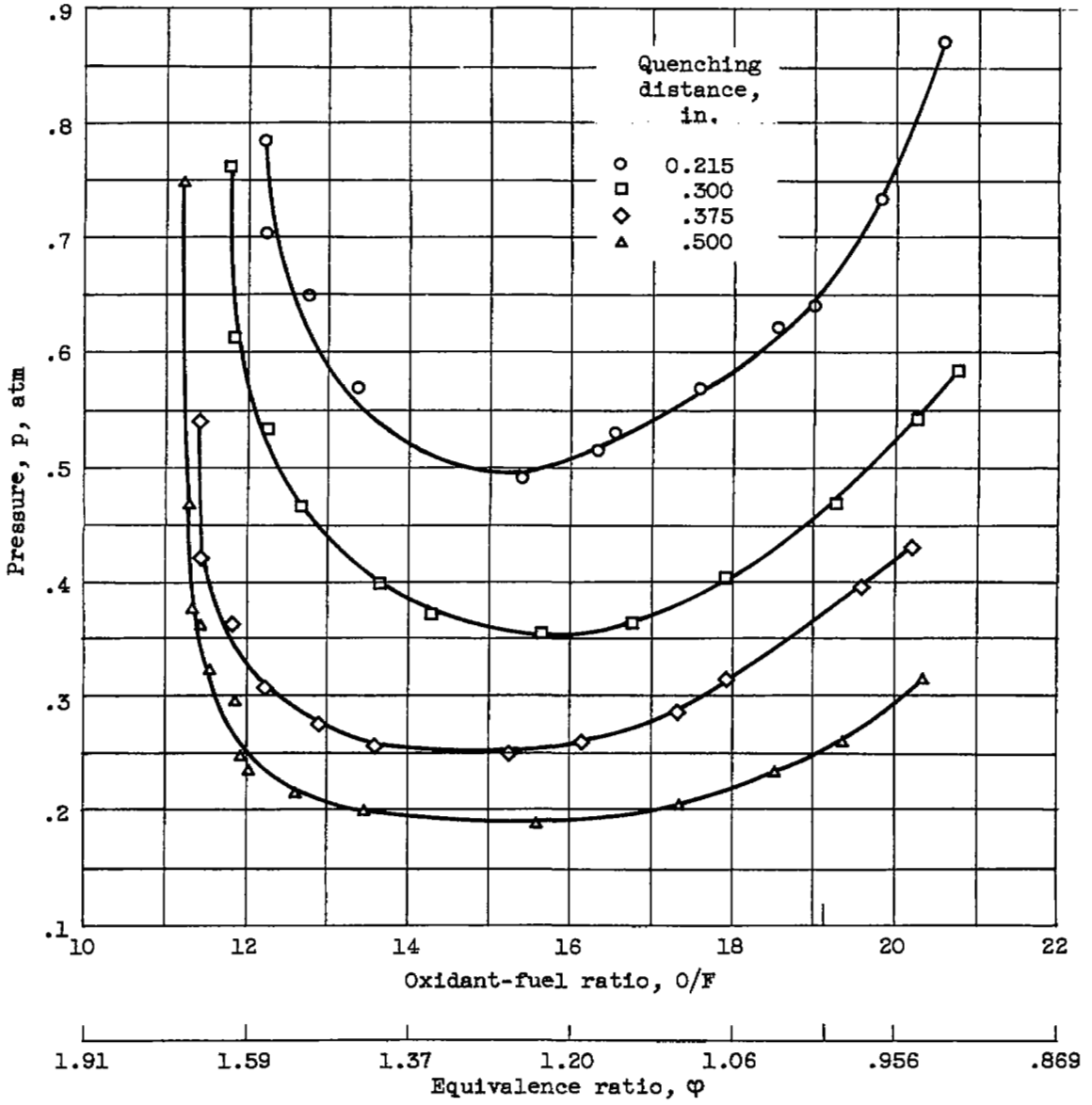

(a) Oxygen fraction, α, 0.17.

Figure 5. - Relation of limiting quenching pressure to O/F and φ for various burner wall separations.

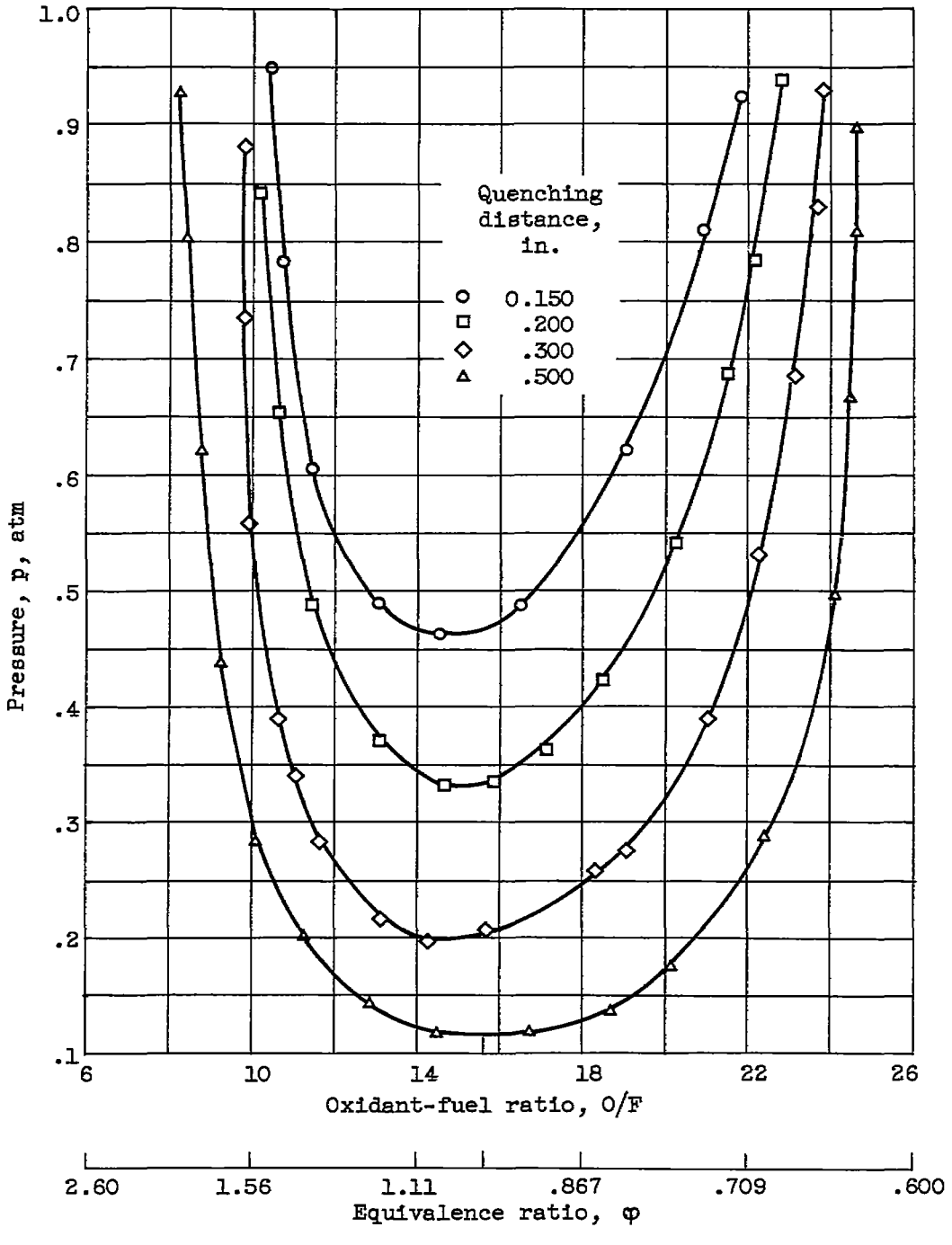

(b) Oxygen fraction, α, 0.21.

Figure 5. - Continued. Relation of limiting quenching pressure to O/F and φ for various burner wall separations.

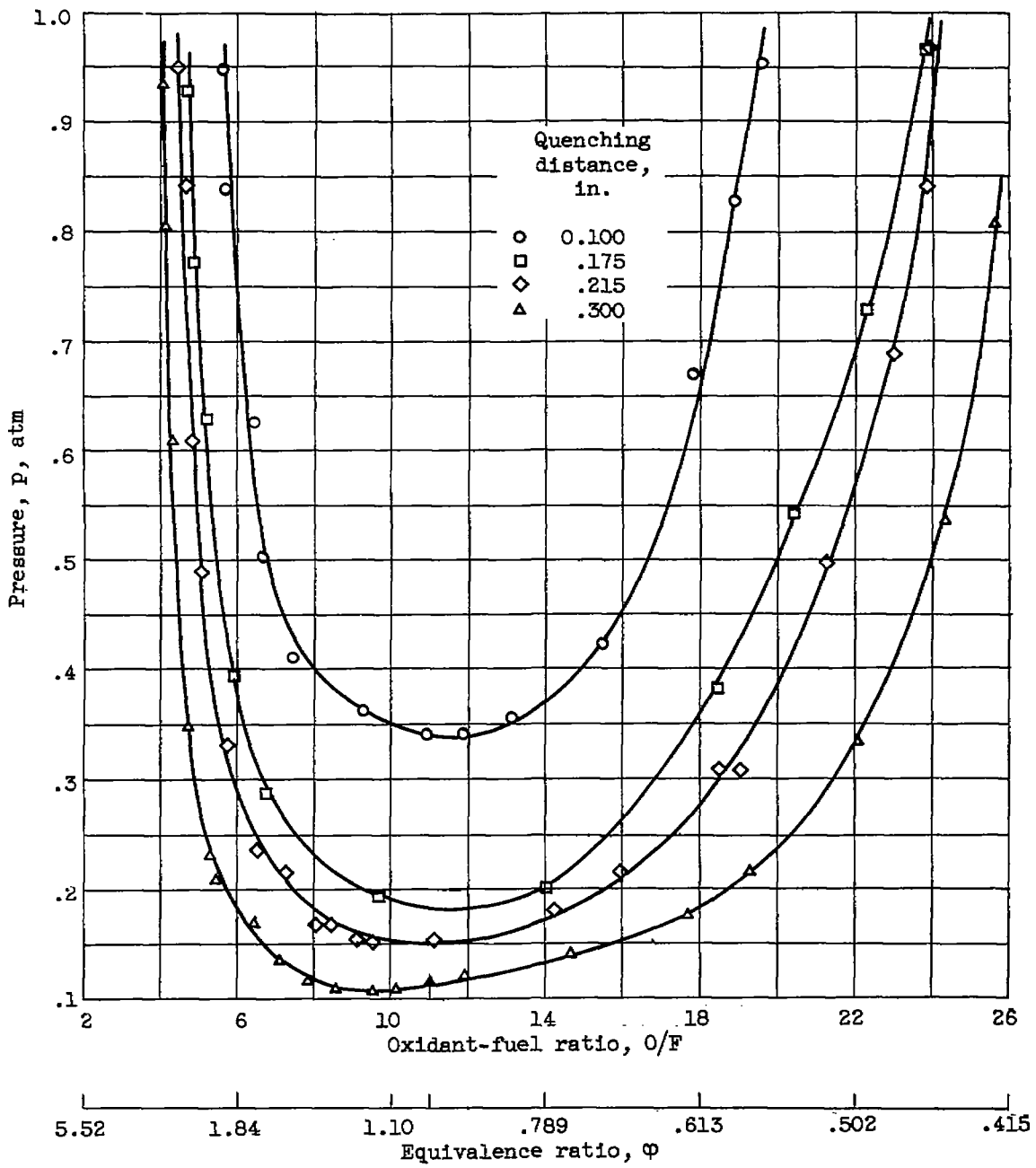

(c) Oxygen fraction, α, 0.30.

Figure 5. - Continued. Relation of limiting quenching pressure to O/F and Φ for various burner wall separations.

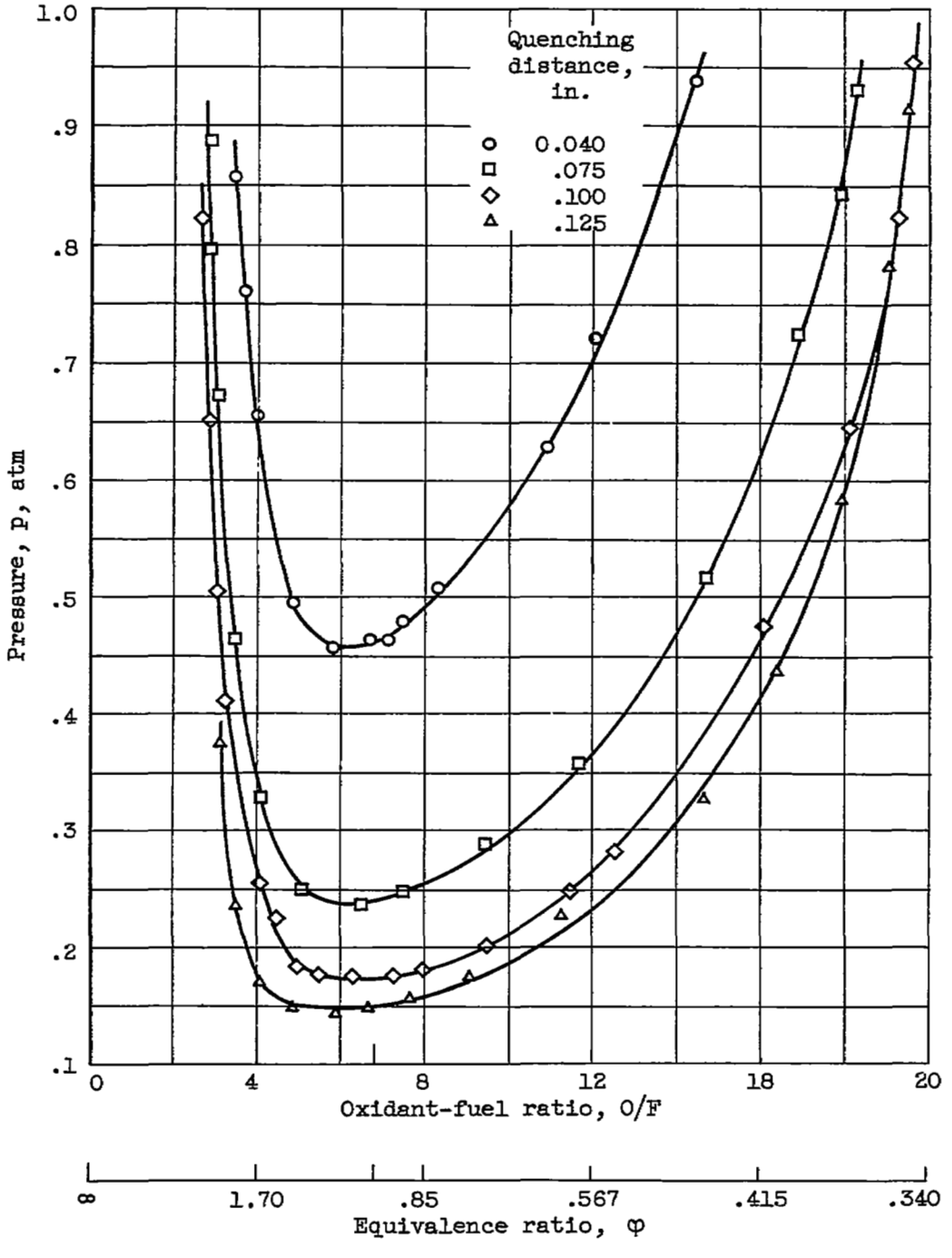

(d) Oxygen fraction, α, 0.50.

Figure 5. - Continued. Relation of limiting quenching pressure to O/F and φ for various burner wall separations.

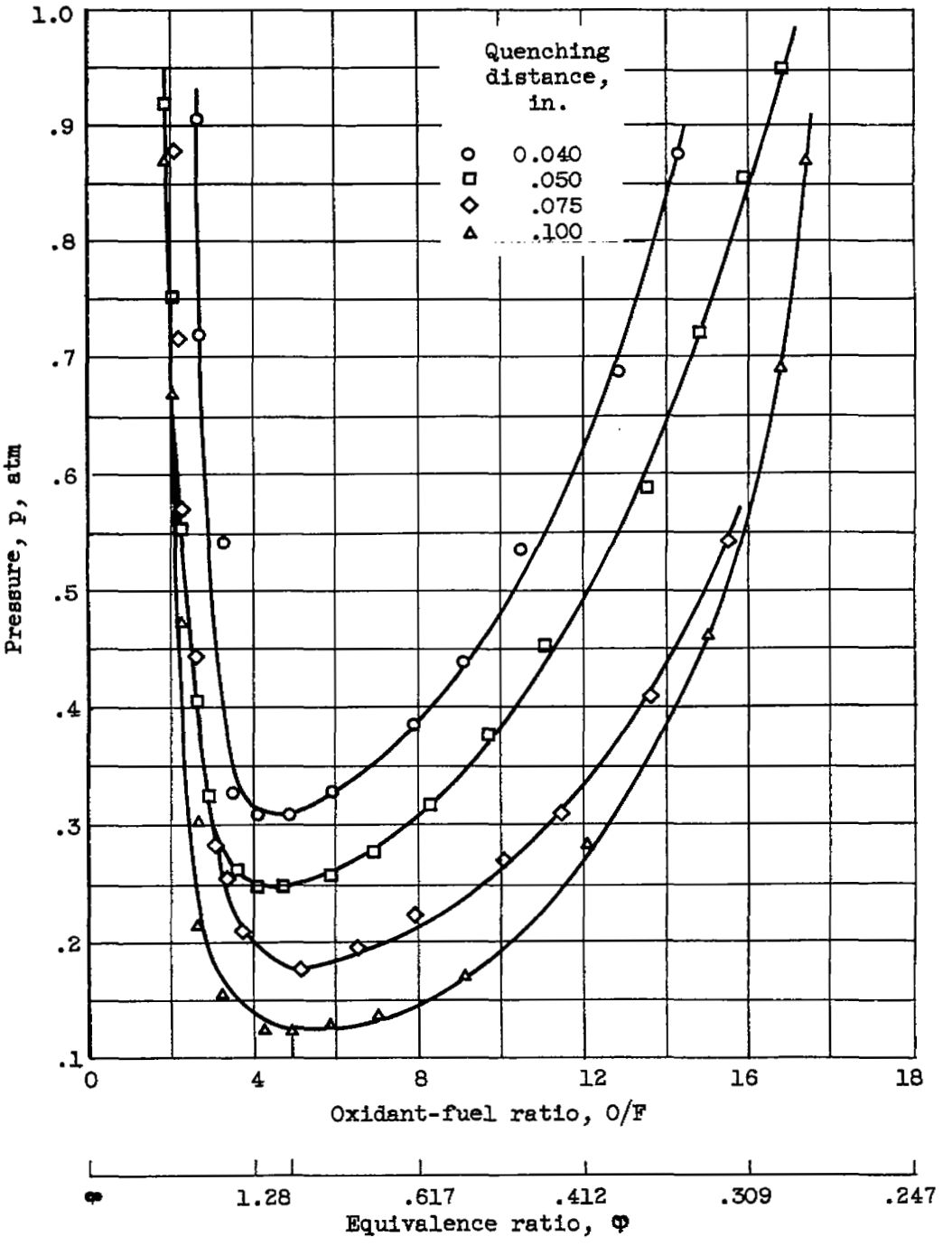

(e) Oxygen fraction, α, 0.70.

Figure 5. - Concluded. Relation of limiting quenching pressure to O/F and φ for various burner wall separations.

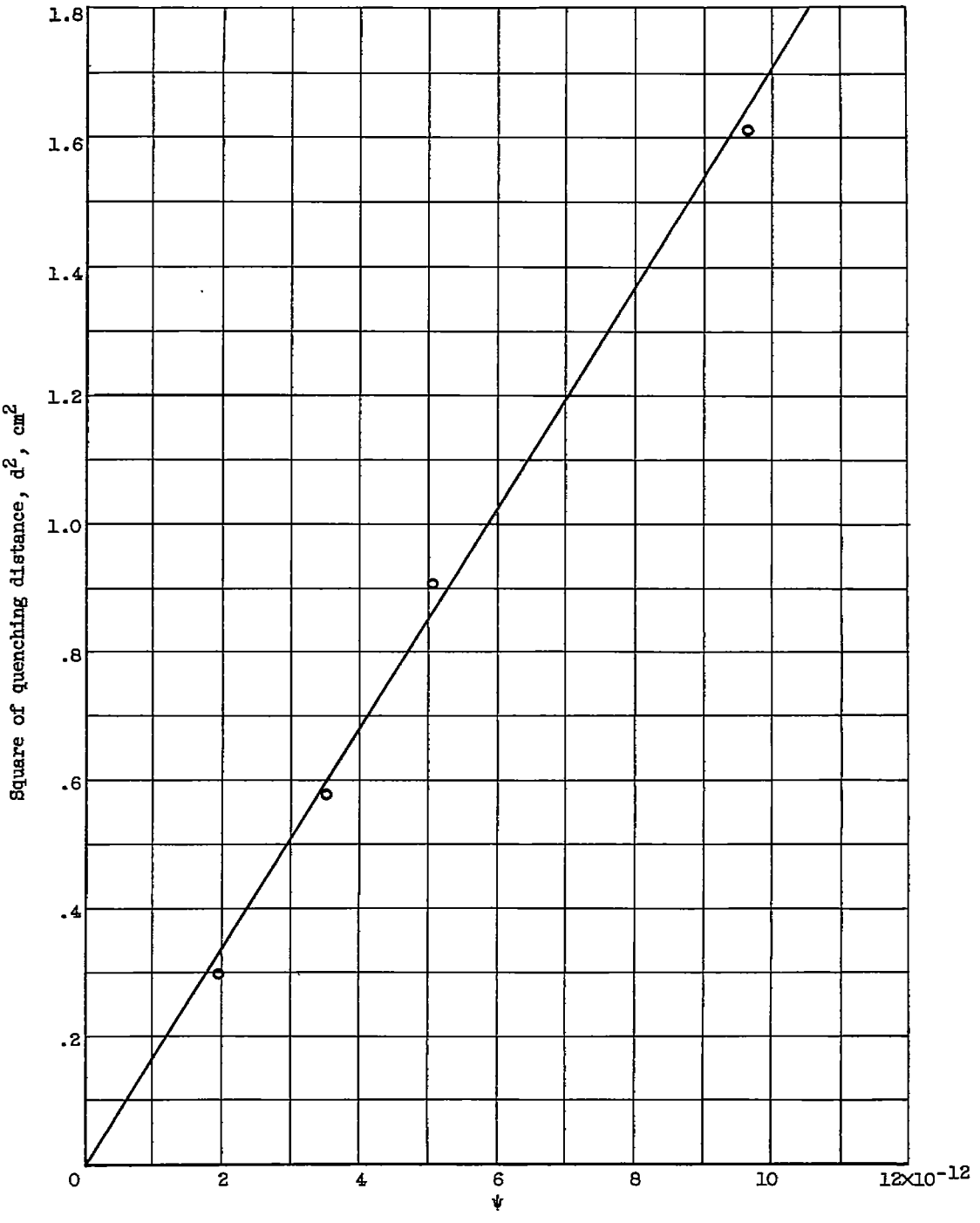

(a) Oxygen fraction, α, 0.17; A/k_1, 0.1694×10^{-12}. Equivalence ratio, φ, 1.00.

Figure 6. - Correlation of experimental data with ψ.

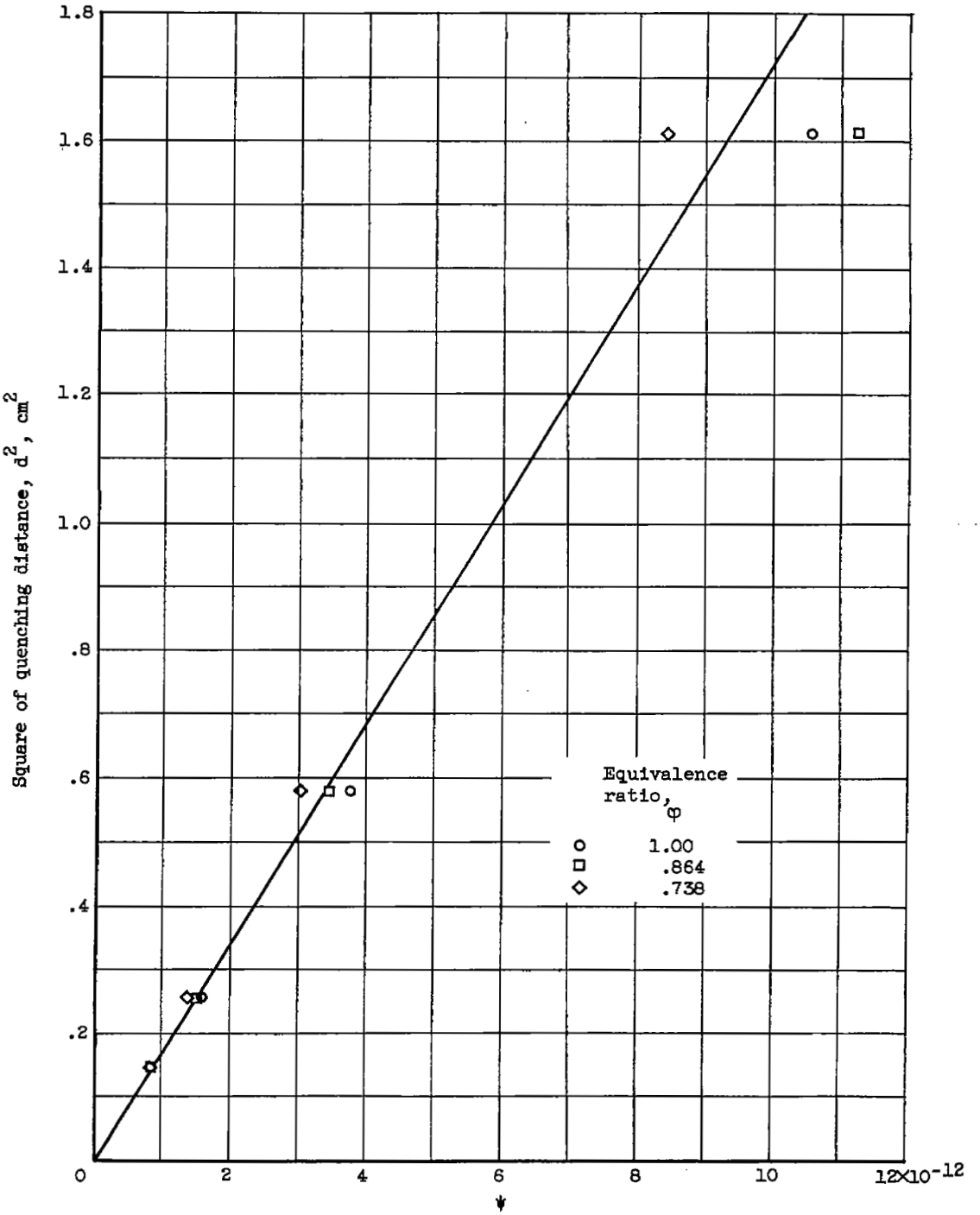

(b) Oxygen fraction, α, 0.21; A/k_1, 0.1737×10^{-12}.

Figure 6. - Continued. Correlation of experimental data with Ψ.

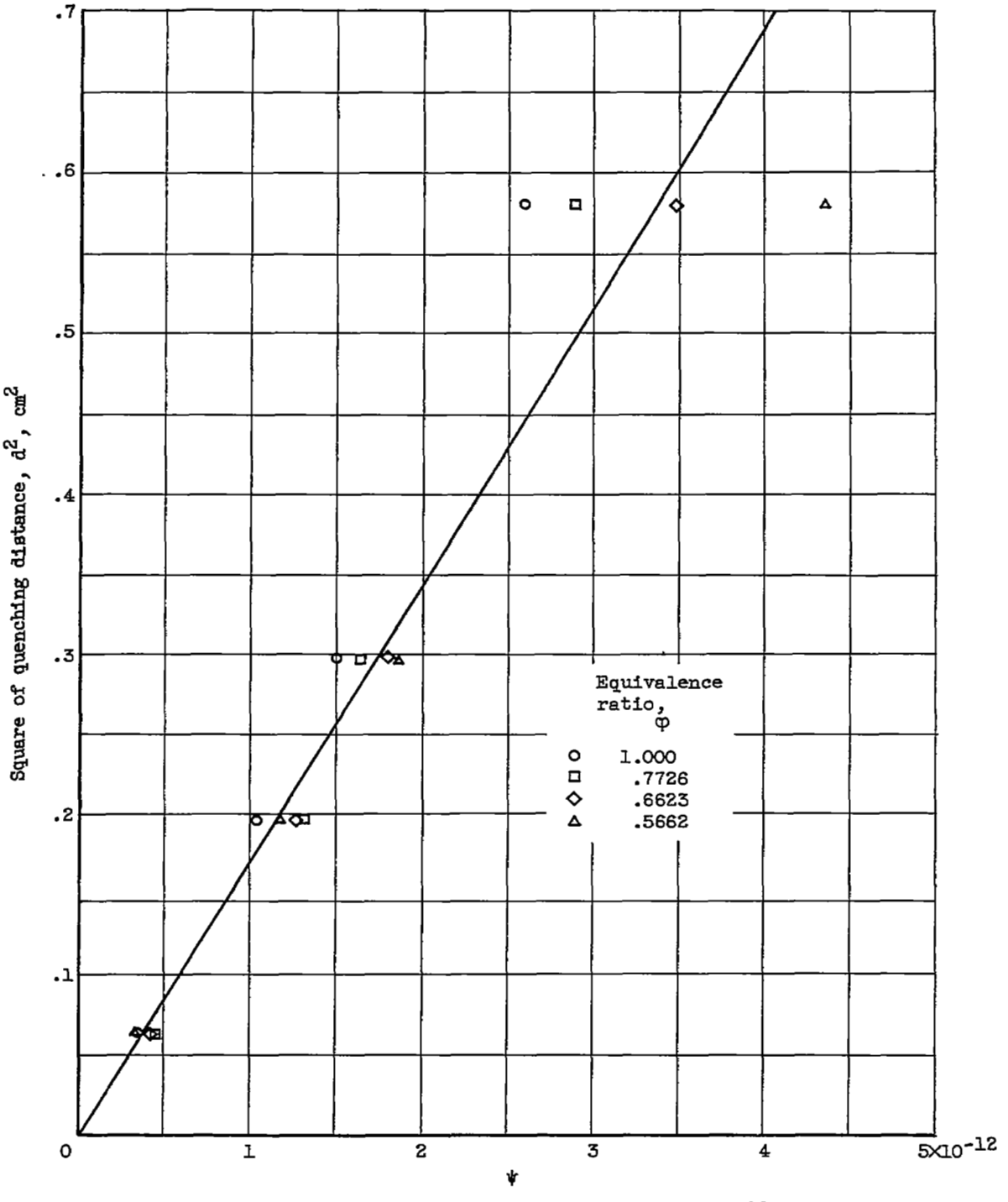

(c) Oxygen fraction, α, 0.30; A/k_1, 0.1751×10^{-12}.

Figure 6. - Continued. Correlation of experimental data with ψ.

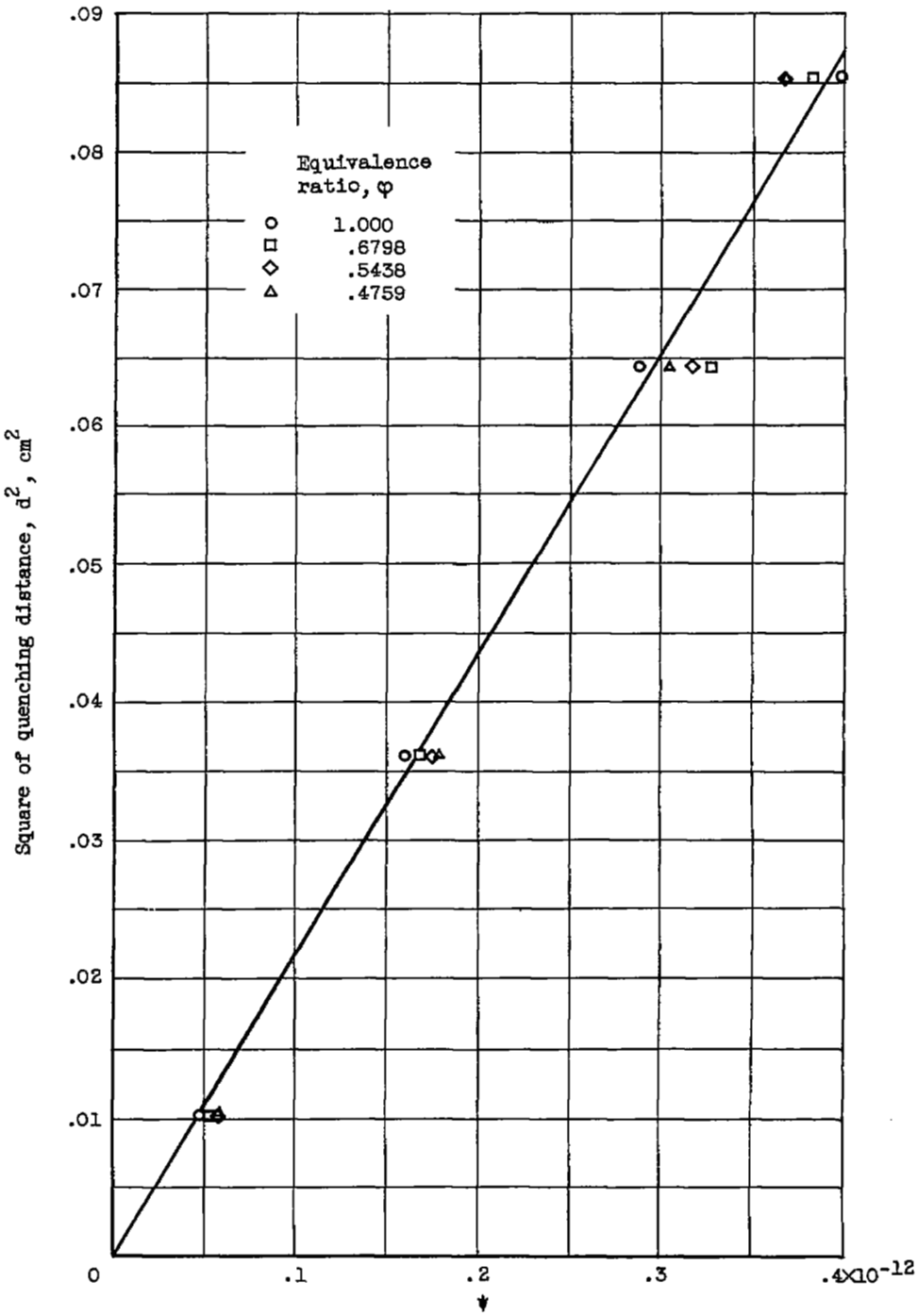

(d) Oxygen fraction, α, 0.50; A/k_1, 0.2205×10^{-12}.

Figure 6. - Continued. Correlation of experimental data with Ψ.

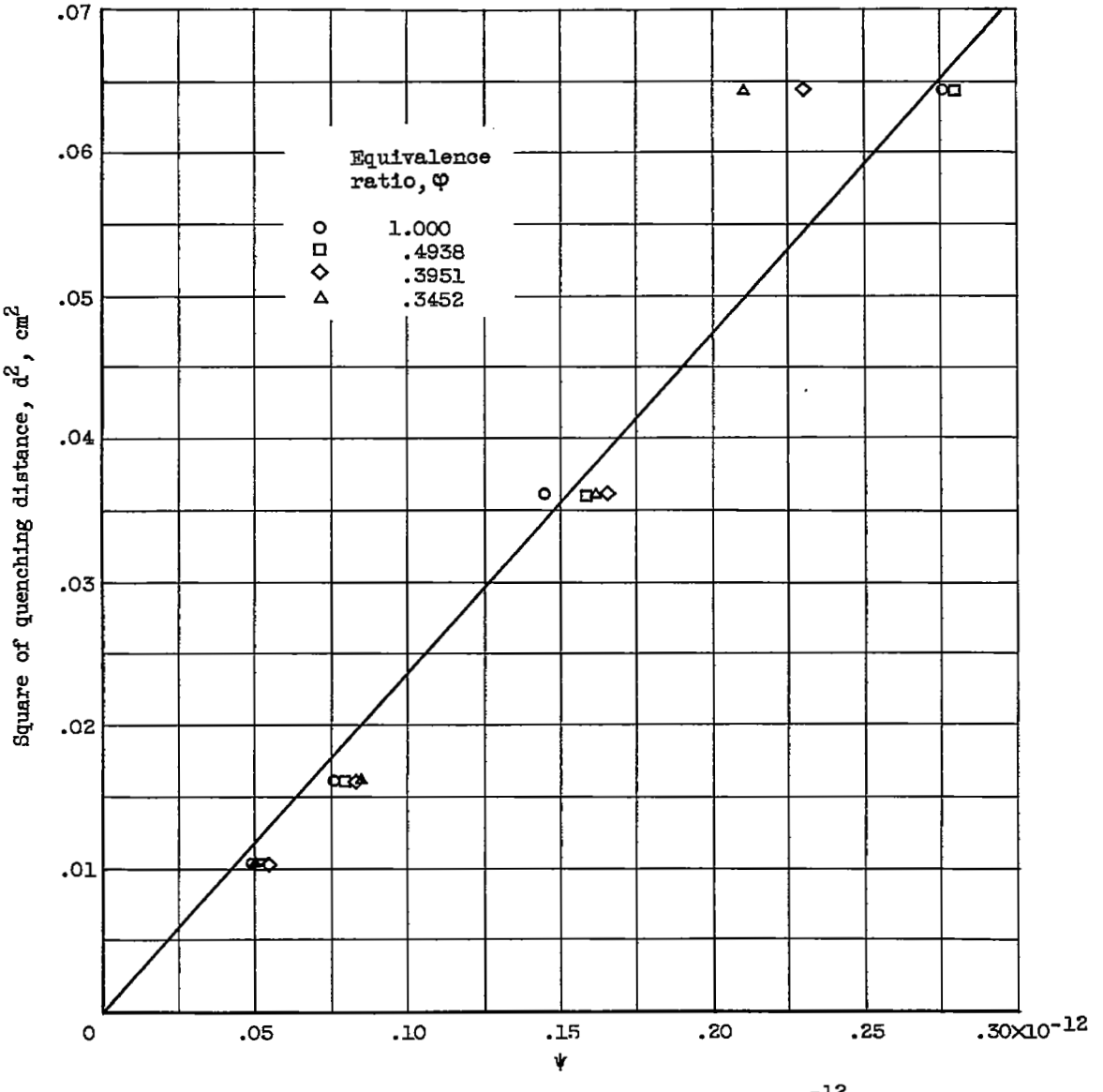

(e) Oxygen fraction, α, 0.70; A/k_1, 0.2360×10^{-12}

Figure 6. - Concluded. Correlation of experimental data with ψ.

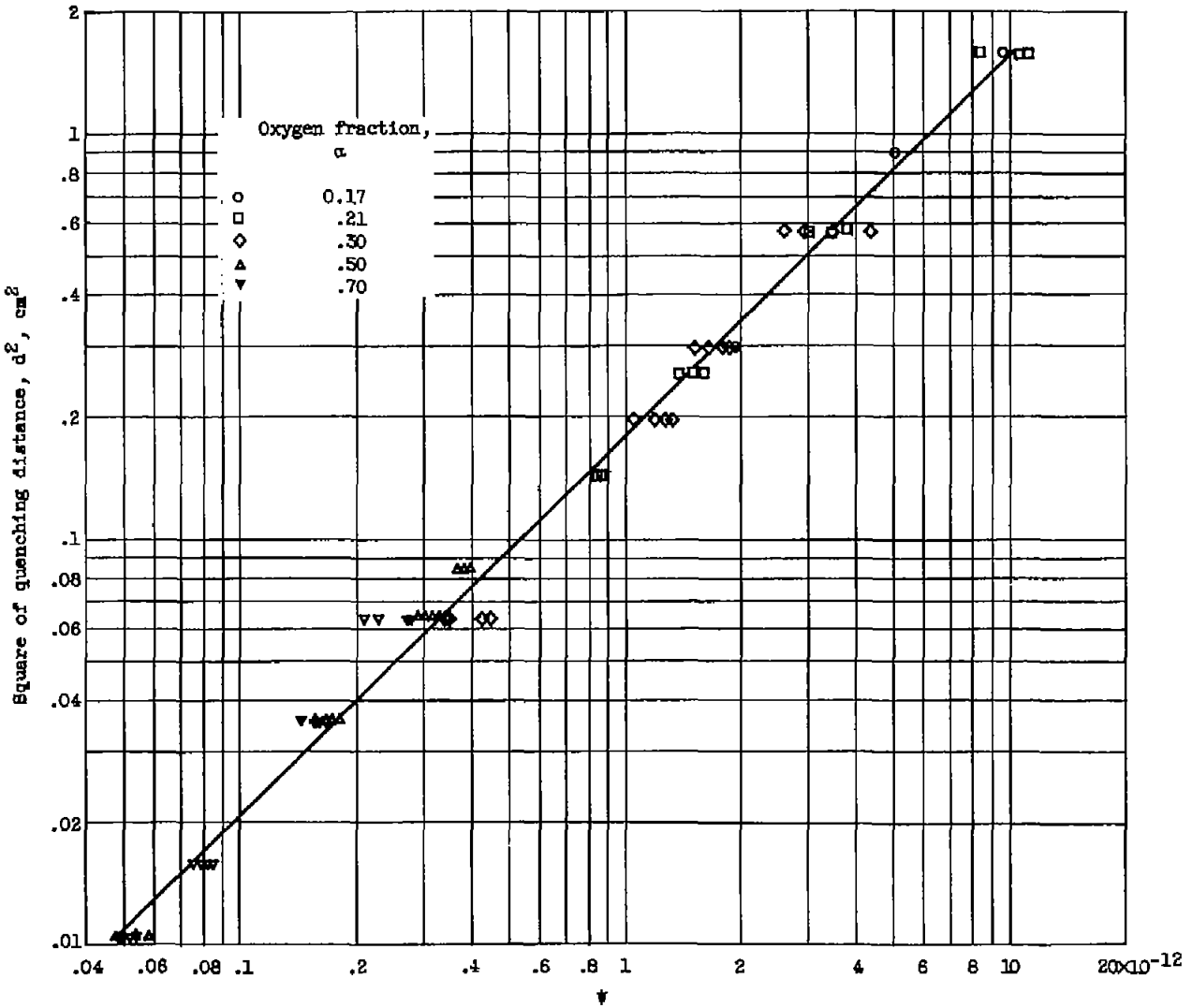

Figure 7. - Correlation of quenching distance data with ψ for all values of oxygen fraction α examined. Equivalence ratio, $\varphi \leq 1.0$.

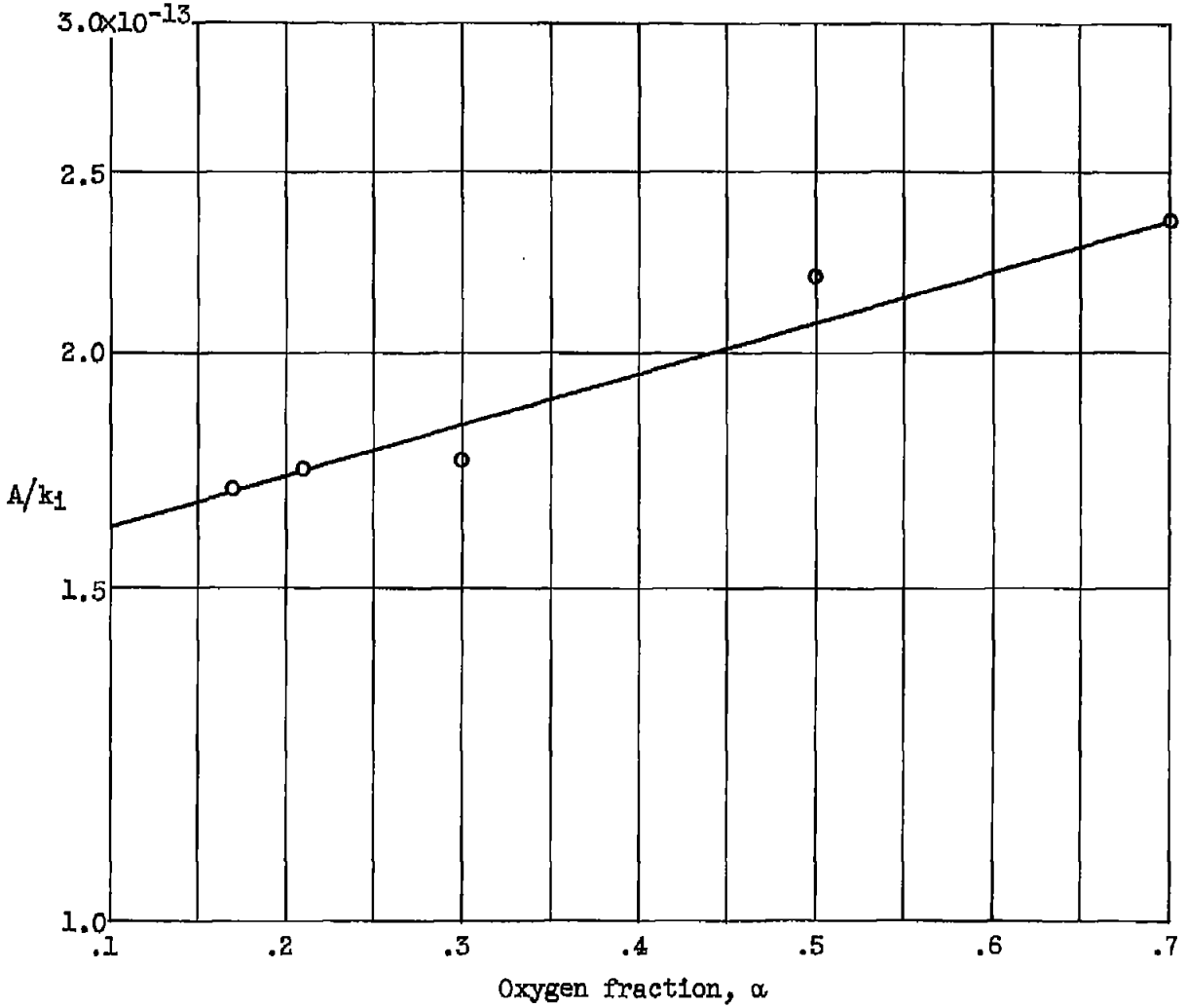

Figure 8. - Variation of A/k_1 with oxygen fraction of oxidant.

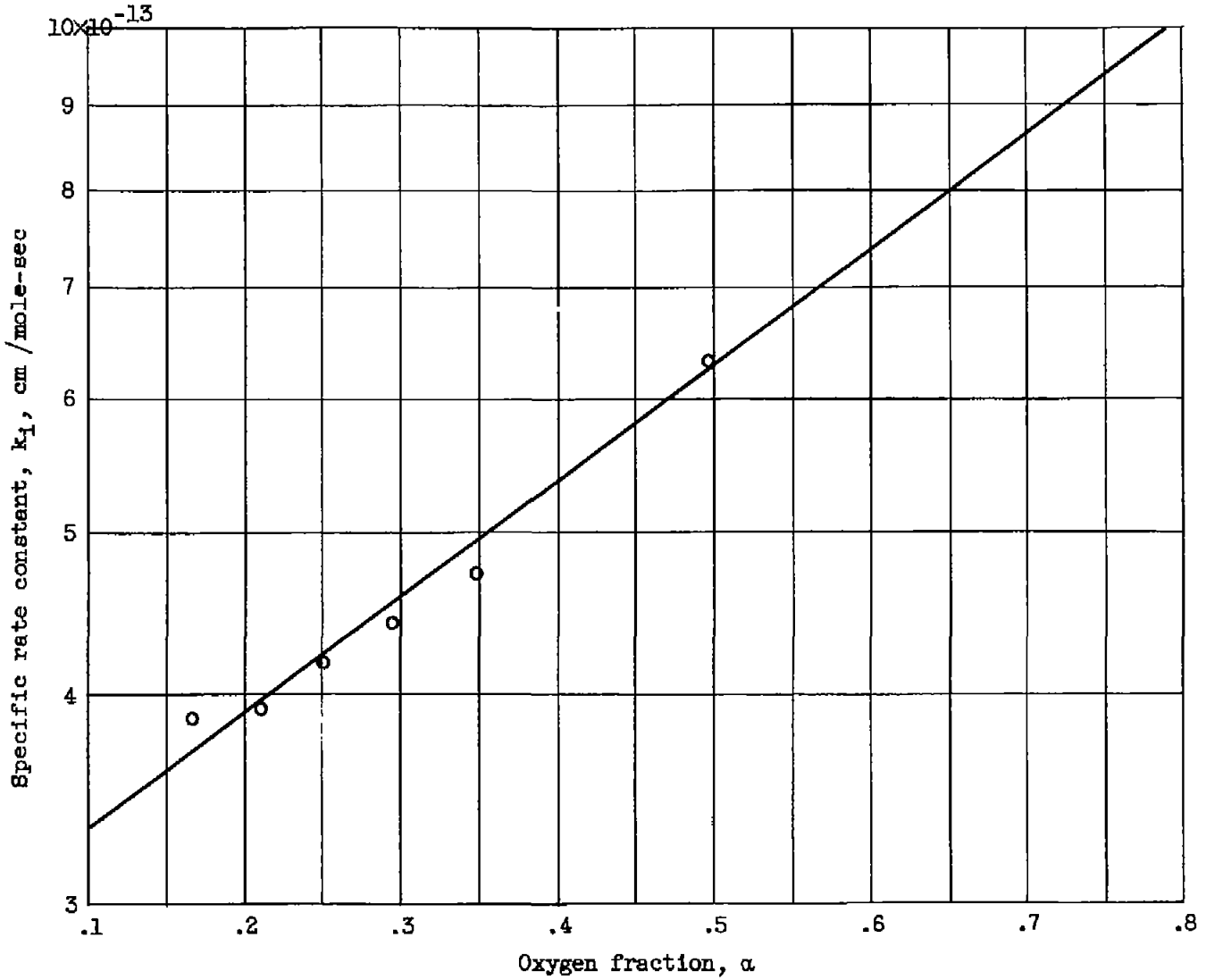

Figure 9. - Variation of specific rate constant with oxygen fraction of oxidant.